AD-A038 412 GEORGE WASHINGTON UNIV WASHINGTON D C INST FOR THE S--ETC F/G 11/6
MECHANICAL PROPERTIES OF ANNEALED AND MARTENSITIC TI-6AL-4V. (A--ETC(U)
AUG 76 C M GILMORE, M A IMAM N00019-76-C-0136
UNCLASSIFIED TR-3 NL

1 OF 1
AD A038412

END

DATE FILMED
5-77

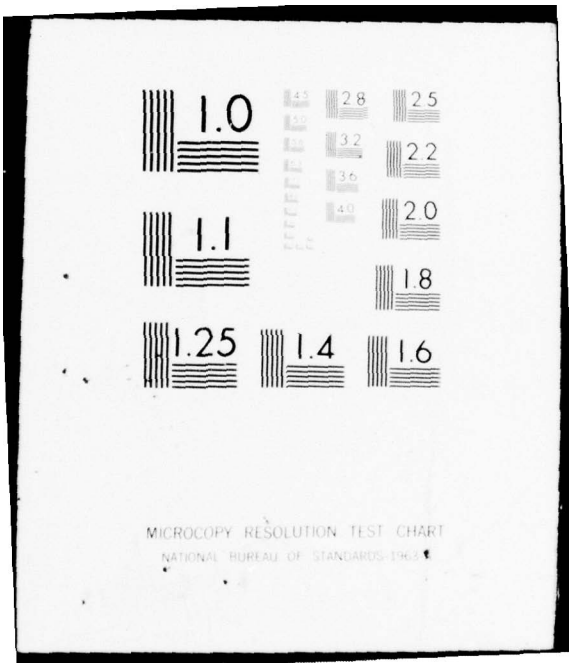
1.0
1.1
1.25
1.4
1.6
2.8
2.5
3.2
2.2
3.6
2.0
4.0
1.8
MICROCOPY RESOLUTION TEST CHART
NATIONAL BUREAU OF STANDARDS-1963

(10)

THE
GEORGE
WASHINGTON
UNIVERSITY

STUDENTS FACULTY STUDY R
ESEARCH DEVELOPMENT FUT
URE CAREER CREATIVITY CC
MMUNITY LEADERSHIP TECH
NOLOGY FRONTIE ESIGN
ENGINEERING APP ENC
GEORGE WASHIN NIV

SCHOOL OF ENGINEERING
AND APPLIED SCIENCE

(10)

INSTITUTE FOR THE STUDY OF FATIGUE, FRACTURE AND STRUCTURAL RELIABILITY

(6)

A. MECHANICAL PROPERTIES OF ANNEALED AND MARTENSITIC Ti-6Al-4V. (A.)

B. MICROSTRUCTURE OF SOLUTION TREATED Ti-6Al-4V. (B.)

C. A STUDY OF FATIGUE DAMAGE WITH ULTRASONIC INTERNAL FRICTION MEASUREMENTS. (C.).

(we letter I)

By

(19) C. M. GILMORE AND M. A. IMAM

SPONSORED BY:

NAVAL AIR SYSTEMS COMMAND

(11) Aug 76

APPROVED FOR PUBLIC RELEASE
DISTRIBUTION UNLIMITED

(12) 67 P.

(15) CONTRACT NO:

N00019-76-C-0136

(9) TECHNICAL REPORT NO.

III

(14) TR-3

SCHOOL OF ENGINEERING AND APPLIED SCIENCE
The George Washington University
Washington, D. C. 20006

405 730 1473

MECHANICAL PROPERTIES OF ANNEALED AND MARTENSITIC Ti-6Aℓ-4V

ABSTRACT

Fatigue life studies are reported on annealed microstructures and on solution treated plus quenched microstructures, and it was found that specimens solution treated at about 900°C (1650°F) had the longest fatigue life, longer by at least a factor of four. A comparison of the α-β annealed alloy with the alloy solution treated at 900°C (1650°F) demonstrated that increases in allowable strain of as much as 50% occurred at high strain amplitude. Annealing and elevated temperature testing appear to decrease the fatigue life of the as quenched alloy. Tensile tests of the alloy solution treated at 900°C showed that this treatment resulted in a high tensile strength and a high ductility (reduction in area) relative to commonly used anneal treatments. Room temperature static load creep tests showed that the alloy solution treated at 900°C had a high elastic limit and a relatively small amount of static creep.

The Mechanical Properties of Annealed and Martensitic Ti-6Aℓ-4V

Introduction

In previous work we have studied the fatigue behaviour of Ti-6Aℓ-4V alloys as a function of their microstructure[1]. A significant result to come from this prior work is the improved fatigue crack initiation life that results in Ti-6Aℓ-4V when it is solution treated at 900°C (1650°F) and water quenched. To supplement this information on fatigue crack initiation life we have conducted other mechanical property tests on both annealed and solution treated Ti-6Aℓ-4V. This paper presents a survey of our results on mechanical properties of heat treated Ti-6Aℓ-4V microstructures. The test results that will be included are: fatigue life at fixed strain amplitude, yield strength, elastic modulus, ultimate tensile strength, ductility, and static load creep. Unfortunately all tests could not be run on the same heat and composition of Ti-6Aℓ-4V alloy, because different specimen shapes required different starting material, which could not always be purchased from the same supplier. Because of this, the chemistry of the specimens used for each test will be reported.

Experimental Tests and Results

A. Fatigue Tests.

Fatigue tests have been conducted on heat treated alloys. The details of the test procedure and specimen preparation were presented previously[1], but some additional tests have been con-

ducted, so the complete results will be presented. For the tests on heat treated alloys solid 1/4 inch diameter rod of the composition given in Table 1 was polished to a 0.1 microinch surface in the reduced center section. The cyclic deformation was fully reversed strair (R=-1), and in addition a small axial stress of 2.12×10^7 N/M^2 (3600 psi) was applied to these specimens so that cyclic creep measurements could also be made. Table 2 gives the results of the fatigue tests at room temperature. The most important result in Table 2 is the significant improvement in fatigue life of the alloy solution treated at 900°C (1650°F). Note that an aging treatment at 760°C (1400°F) for 1 hour destroys the improved fatigue life observed in the solution treated alloy.

Table 2 shows the improved fatigue life at a fixed strain; in addition, it is often important to know the increase in allowable strain (or stress) at a fixed number of cycles. This can be found from the strain amplitude $\overline{vs}$ cycles to failure diagram shown in Figure 1 for an α-β anneal and 900°C (1650°F) solution treatment. For example, at 9×10^3 cycles to failure, the alternating shear strain amplitude is about 20×10^{-3} for the alloy solution treated at 900°C (1650°F), and for the α-β annealed alloy the alternating strain amplitude was 13×10^{-3} for 9×10^3 cycles to failure. This is more than a 50% increase in the allowable shear strain level. From Figure 1 it appears that at high strain amplitudes, the alloy solution treated at 900°C (1650°F) will show even larger percentage increases in allowable strain relative to the annealed state.

Titanium alloys are often used in elevated temperature applications, thus elevated temperature fatigue tests will give some indication of the thermal stability of the alloy. Table 3 gives the results of fatigue tests conducted at 260°C (500°F) under the same conditions as the tests reported in Table 2. The alloy solution treated at 900°C (1650°F) still has a longer fatigue life than the α-β anneal, but the factor is not as large as it was at room temperature. Note that the fatigue life of the α-β anneal alloy increased in going from room temperature (Table 2) to the elevated temperature; where as, the fatigue life of the alloy solution treated at 900°C (1650°F) decreased. It appears that at elevated temperatures, the fatigue lives of the two treatments are approaching each other.

B. Tensile Tests

Tensile tests were performed on annealed microstructures and the microstructure solution treated at 900°C (1650°F). The chemical composition of the alloy used for these tests is given in Table 4. Several different annealing procedures were utilized in this experiment and these procedures are listed below:

α-β Anneal (αβA)

800°C (1472°F) for 3 hours, furnace cool (FC) to 600°C (1112°F), followed by air cool (AC) to room temperature.

Recrystallization Anneal (RA)

928°C (1702°F) for 4 hours, FC to 760°C (1400°F) at 180°C/hour, FC to 482°C (900 F) at 372°C (702°F)/hour, AC.

β Anneal

0.5 hour at 1037°C (1900°F), AC to room temperature, 732°C (1350°F) for 2 hours, AC to room temperature.

The annealing was all done in a vacuum of at least 10^{-5} torr. The solution treatment at 900°C was performed in a vertical air furnace, two solution times are reported 10 min. and 15 min.; the specimens were then water quenched. The specimens were nominally 1.27 cm. diamater with a 8.26 cm. gage length. The tensile tests were conducted in a Materials Testing System.

The experimental results are presented in Table 5, and Figure 2 is a photograph of four fractured specimens. The

specimen solution treated at 900°C had yield and tensile strengths significantly higher than the α-β anneal and the RA, but the strengths of the β-anneal are higher. The tensile properties of the β-anneal from this test are in good agreement with the results of Harrigan et al[2], but there appears to be a wide range of properties in the literature for the β-anneal alloy. Note also that the β-anneal treatment resulted in the lowest ductility of all the treatments. The alloy solution treated at 900°C (1650°F) appears to have a good balance of tensile properties, ie the maximum ultimate tensile strength observed with the ductility (reduction in area) being the maximum; the α-β anneal and the 1650°F solution treatment had essentially equal ductility. The elastic modulus listed in Table 5 was obtained by measuring the slope of the stress strain diagram.

C. Static Creep

It has been observed by numerous authors that titanium alloys can creep at room temperature when subject to stresses that are only a fraction of the yield stress. Some titanium alloys appear to be elastic up to some limit stress, that is only a small fraction of yield, then they exhibit a combination of elastic plus plastic behavior up to the yield point, then some of titanium alloys are known to exhibit extensive creep with little apparent strain hardening. A static creep test can show the true elastic limit, the amount of plastic creep below yield, and it can give an indication of strain hardening after the yield stress has been exceeded.

A schematic of the test facility utilized for the creep test is shown in figure 3. A static weight is applied to a pulley that converts the load into a torque about the specimen axis. The strain is measured with two mirrors that are attached to flats on brass collars that attach to the specimen. Attaching the mirrors to the specimen eliminates the possibility of recording any grip slippage as specimen strain. The collars are each attached to the specimen with three conical set screws spaced at 120° around the specimen. Only the set screws touch the specimen, and thus the spacing between the set screws of the two mirrors determines the gage length. The collars are machined so that the gage length is always one inch. The twist strain is measured by determining the relative change in tilt of the two mirrors. By taking the relative tilt of the two mirrors any slippage in the grips is eliminated from the measurement. The relative tilt

angles are determined by using a laser source of light and collimating it to get a line. The single line is split by the two mirrors and each beam is reflected to a circular scale one meter from the specimen. The laser source provides a sharp bright image in comparison with the incandescent sources we have tried. We estimate that we can measure shear strain as low as 2×10^{-5} with this device. In these tests our procedure was to measure the strain until no additional strain could be detected in a 24 hour period. Then the load was increased by an increment. The loading was continued until the specimen yielded. The total strain at yield was also recorded. In this report the static creep of an alloy of Ti-6Aℓ-4V will be determined for a specimen solution treated at 900°C (1650°F) in a sealed evacuated vycor tube and water quenched with the tube being broken during quenching. The results will be compared with previously presented results on annealed microstructures[3]. The annealed microstructures to be used are recrystallize anneal (RA), β anneal and α-β anneal. The details for these annealing procedures were presented in the section on tensile testing. The specimens for this test are thin walled tubes with an outside diameter of .635 cm (.25 in.) and an inside diameter of .538 cm (.212 in.). The thin wall is necessary in a torsion test to obtain a section with as uniform a strain field as possible. If a solid rod was used then the center of the rod would be under no strain and the outer surface of the rod would be under maximum strain. The tubes are seamless extruded Ti-6Aℓ-4V with the composition shown in table 6.

Results and Discussion of Static Creep Tests.

Stress strain diagrams for each of the treatments are shown in figures 4 to 7. In addition, the detailed measurements at each load are presented in Appendix A. The initial stressing was done in increments of 3.2×10^7 N/M^2 (4747 psi) until transient creep was observed; then the stress was increased in increments of 8.18×10^7 (11868 psi). Thus the elastic limit, defined as the maximum stress where no transient creep is observed, is only known to within $^{+0}_{-3.2 \times 10^7}$ N/M^2 ($^{+0}_{-4747}$ psi). The results from the determination of the elastic limit are summarized in table 7. The observed elastic limits for unidirectional loading show that the alloy solution treated at 900°C (1650°F) and water quenched has the highest elastic limit; whereas, the β annealed alloy which has demonstrated the shortest fatigue lives has the lowest elastic limit. This correlation between elastic limit and fatigue life is most interesting. Note also that the elastic limit and the yield point do not show any correlation; for example, the β annealed alloy has the highest yield point but the lowest elastic limit. After the elastic limit is surpassed, the β annealed alloy has the smallest amount of transient creep. The results of creep versus time in figure 8 at 4.9×10^8 N/M^2 (71.211 KSI) most clearly demonstrate that the smallest creep strain occurs in the β annealed alloy. The alloy solution treated at 900°C had the next lowest creep rates, and the recrystallized anneal alloy had the highest creep rate.

Summary and Conclusions

The above sections provided a summary of some mechanical properties of the alloy Ti-6Aℓ-4V solution treated at 900°C (1650°F) and water quenched; these results were compared with the mechanical properties of annealed microstructures. The alloy solution treated at 900°C and water quenched has significantly improved fatigue properties relative to the annealed microstructures. For the other tests that were conducted, the solution treated alloy had properties comparable to the annealed microstructures, but in all of the tests, the properties of the solution treated alloy could be rated as good in relation to some of the anneal treatments. For example, in the tensile test, the solution treated alloy had both a high yield and ultimate strength and high ductility, whereas, the α-β annealed and recrystallized anneal alloys had low yield and ultimate strength but high ductility. Conversely, the β annealed alloy had a high yield strength, but a very low ductility. Also, the solution treated alloy had the highest elastic limit and it demonstrated an intermediate amount of creep. Only the β annealed alloy had less creep strain; however, the β annealed alloy also had the lowest elastic limit. Thus, for an application which is fatigue sensitive, solution treating the alloy might provide a desirable combination of properties. However, other properties such as stress corrosion resistance, crack propagation, and fracture toughness have yet to be determined.

In another paper we have discussed the microstructural changes that cause the improved fatigue properties in solution treated alloys.

REFERENCES

1. M. A. Imam and C. M. Gilmore, Fatigue Life in Annealed and Martensitic Ti-6Aℓ-4V, Institute for the Study of Fatigue, Fracture and Structural Reliability, Report IIB, for contract N00019-75-C-0093 to Naval Air Systems Command, August 1975.

2. M. J. Harrigan, M. P. Kaplan and A. W. Sommer, Fracture Prevention and Control, A.S.M. Materials/Metal Working Series No. 3, 1974, pg. 225.

3. M. A. Imam and C. M. Gilmore, Room Temperature Creep of Ti-6Aℓ-4V, Institute for Fatigue, Fracture, and Structural Reliability Report 25, May 1976.

Table 1

Chemical Composition of Ti-6Aℓ-4V Used for Solid Rod Torsion Specimens in Weight Percent

Aℓ	V	O	H	C	N	Fe
6.4	4.0	.141	55 ppm	.01	.014	.18

β Transus 980°C (1805°F)

Table 2

FATIGUE LIVES OF HEAT TREATED Ti-6Al-4V ALLOYS CYCLED AT A SHEAR STRAIN OF ±0.02 PLUS AN AXIAL STRESS OF 2.12×10^7 N/M^2

HEAT TREATMENT†	MEAN*	MINIMUM	STANDARD DEVIATION
α-β ANNEAL	944	429	443
843°C (1550°F)ST + WQ	2497	1837	717
900°C(1650°F)ST +WQ	9616	8917	758
1065°C(1950°F)ST +WQ	2396	1633	487
900°C(1650°F)ST +WQ+760°C(1400°F) 1 hr.	852	745	122

*Results based upon four specimens for each heat treatment.

† ST-solution treatment for 10 minutes
WQ - Water Quench

α-β Anneal - 800°C (1472°F) for 3 hours, furnace cool to 600°C (1112°F), Air cool to room temperature.

TABLE 3

FATIGUE LIVES OF HEAT TREATED
Ti-6Aℓ-4V ALLOYS CYCLED AT A
SHEAR STRAIN OF ±0.02 AT 500°F

HEAT TREATMENT	MEAN	MINIMUM	STANDARD DEVIATION
α-β ANNEAL	1987	1557	894
900°C (1650°F)ST + WQ	4818	4090	634

TABLE 4

CHEMICAL COMPOSITION OF Ti-6Aℓ-4V
ALLOY USED FOR TENSILE TESTS IN
WEIGHT PERCENT

Aℓ	V	O	Fe	N	C	H
6.3	4.2	.188	.17	.010	.02	67ppM

TABLE 5

TENSILE TEST RESULTS FOR Ti-6Aℓ-4V

THERMAL TREATMENT	YIELD STRENGTH 10^8 N/m^2 (ksi)	ULTIMATE STRENGTH 10^8 N/m^2 (ksi)	YOUNG'S MODULUS 10^{11} N/m^2 (10^7 psi)	PERCENTAGE REDUCTION IN AREA	PERCENTAGE ELONGATION
S.T.-10 min. 900°C + W.Q.	9.99 (144.9)	11.59 (168.1)	1.20 (1.74)	39.8	26.0
S.T.-15 min. 900°C + W.Q.	9.96 (144.5)	11.56 (167.7)	1.12 (1.62)	40.6	27.0
α-β Anneal	8.99 (130.46)	9.90 (143.6)	1.03 (1.50)	41.0	30
RA	8.65 (125.4)	9.69 (140.6)	1.24 (1.80)	34.4	24.9
β-Anneal	10.38 (150.6)	10.78 (156.5)	1.25 (1.82)	9.08	12.5

TABLE 6

CHEMICAL COMPOSITION OF Ti-6Aℓ-4V
THIN WALLED TUBE

Aℓ	V	O	Fe	N	C	H
5.8	4.4	.113	.08	.01	.02	69 ppM

TABLE 7

ELASTIC LIMITS OF Ti-6Aℓ-4V ALLOYS
DETERMINED FROM STATIC CREEP EXPERIMENTS

THERMAL TREATMENT	ELASTIC LIMIT N/M^2 (psi)
RA	12.8×10^7 (18,990)
$\alpha\beta$A	12.8×10^7 (18,990)
βA	9.6×10^7 (14,242)
900°C S.T. + W.Q.	15.0×10^7 (23,737)

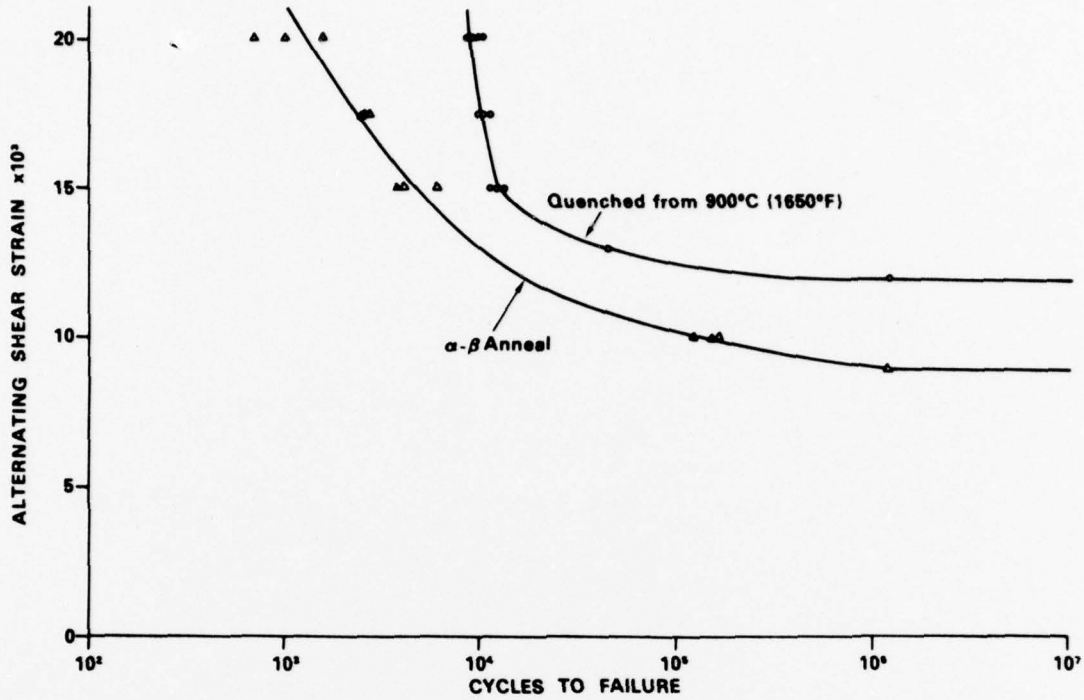

Figure 1. Cycles to failure as a function of the applied alternating shear strain for specimens α-β annealed and solution treated at 900°C and water quenched

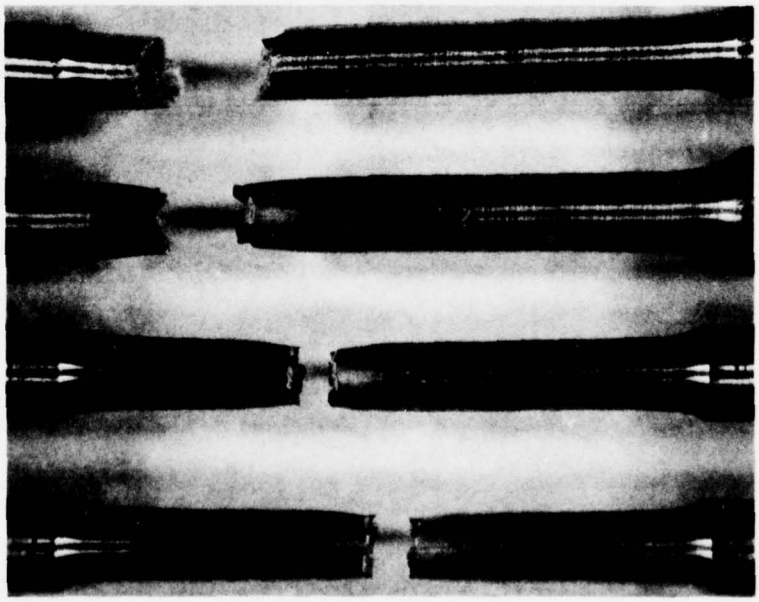

Figure 2. Tensile test specimens showing reduction in area and elongation for the following heat treatments from top to bottom: β anneal, 900°C solution treatment plus water quench, α-β anneal, recrystallize anneal.

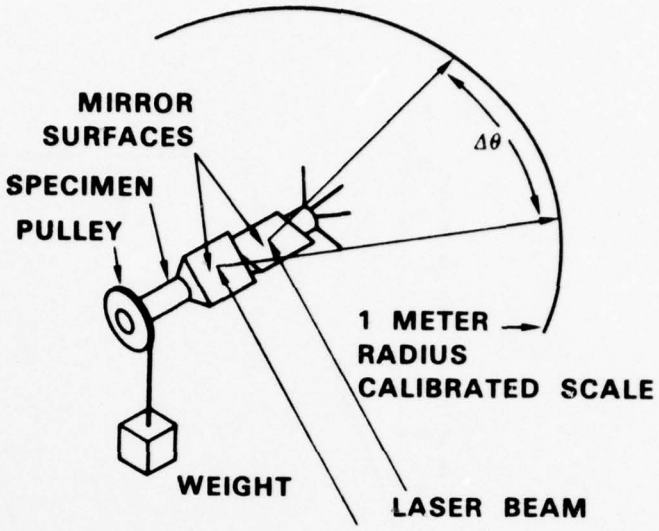

Figure 3. Schematic of the static torsion creep facility. The shear stress is applied to the tubular specimen by a weight attached to a pulley. The specimen is clamped in a pair of grips; the front grip is rotatable, and the rear grip is fixed. Two mirrors are attached to the specimen by three conical set screws at 120° separation for each mirror; the distance between the attachment screws is the 1 inch gage length. The relative tilt between the two mirrors is measured with a single laser beam that is split by the two mirrors and reflected to a 1 meter radius calibrated scale.

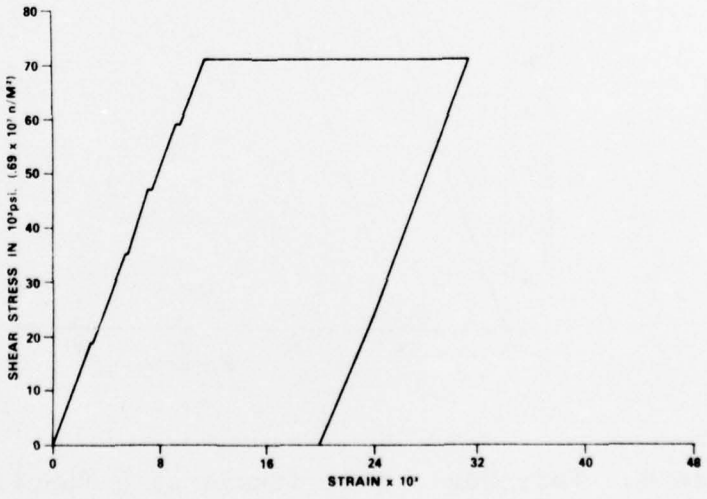

Figure 4. Torsional strain as a function of applied shear stress for α-β annealed Ti-6Aℓ-4V. The strain steps are the accumulation of creep strain at a constant sustained shear stress.

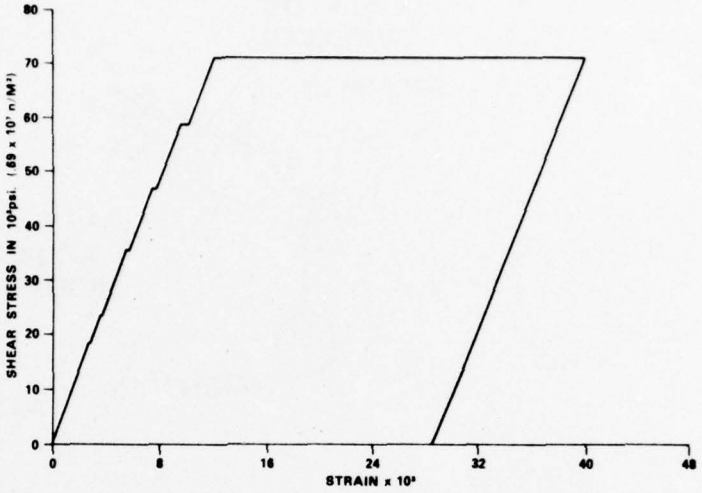

Figure 5. Torsional shear strain as a function of applied shear stress for recrystallized anneal Ti-6Aℓ-4V.

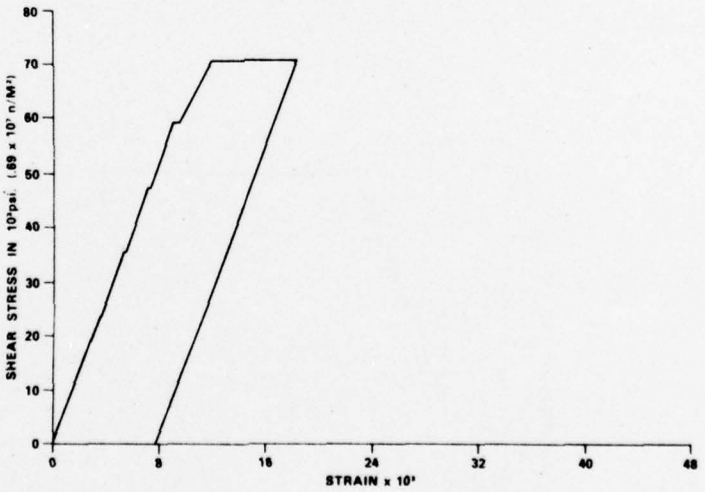

Figure 6. Torsional shear strain as a function of applied shear stress for β annealed Ti-6Aℓ-4V.

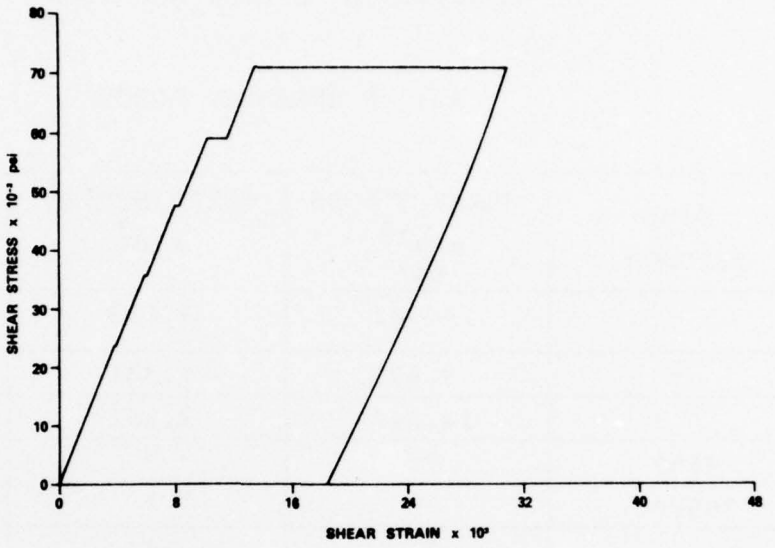

Figure 7. Torsional shear strain as a function of applied shear stress for Ti-6Aℓ-4V solution treated at 900°C and water quenched.

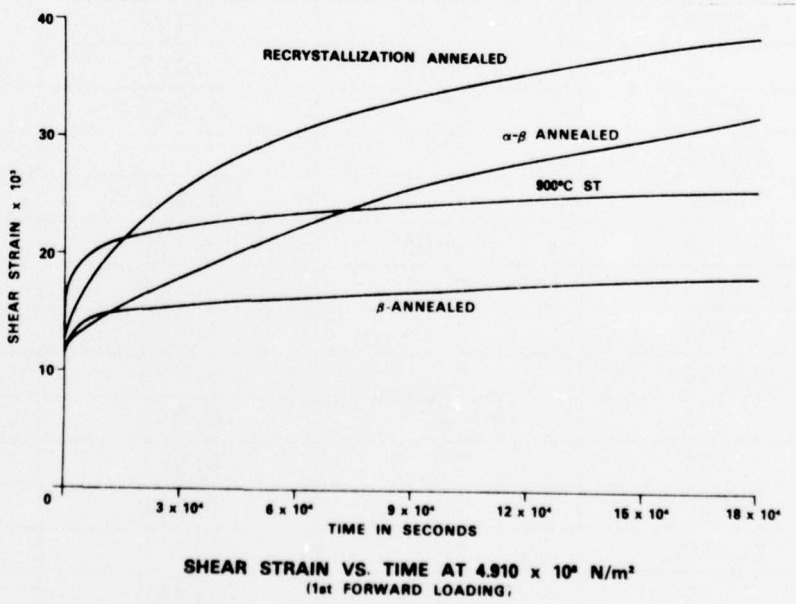

Figure 8. Shear strain as a function of time at a shear stress of 4.91×10^8 N/M^2 for the heat treatments shown. This is for initial unidirectional loading.

APPENDIX A

SHEAR STRAIN AS A

FUNCTION OF STRESS AND TIME

- * -

A.1 β ANNEALED ALLOY

TIME SECONDS	SHEAR STRESS $x10^{-3}$ psi	SHEAR STRAIN $x10^{3}$	REMARKS
-	4.747	0.655	No Creep
-	9.495	1.331	No Creep
0	14.242	2.051	
4650	"	"	
76650	"	"	
	"	"	
0	-	2.400	
72000	"	"	
0	18.9896	2.771	
4090	"	"	
68680	"	2.792	
0	23.737	3.447	
19720	"	3.469	
32600	"	"	
87240	"	3.490	
0	35.606	5.170	
3330	"	5.192	
12850	"	5.214	
24240	"	5.279	
0	47.474	6.937	
200	"	6.981	
30860	"	7.090	
83890	"	"	
0	59.343	8.988	
1750	"	9.097	
2600	"	"	
78360	"	9.381	

A.1 Continued

TIME SECONDS	SHEAR STRESS $x10^{-3}$ psi	SHEAR STRAIN $x10^{3}$	REMARKS
0	71.211	11.06	
100	"	12.369	
2010	"	13.722	
7400	"	14.616	
18600	"	15.511	
23960	"	15.772	
31480	"	16.012	
46140	"	16.427	
87220	"	17.147	
97610	"	17.256	
107460	"	17.408	
125160	"	17.670	
175000	"	18.107	
	59.343	16.427	
	47.474	14.682	
	35.606	13.002	
	23.737	11.257	
	14.242	9.795	
	4.747	8.377	
0	0	7.657	
6640	"	7.635	Creep recovery
16630	"	"	"
88030	"	7.613	"
after 22 hrs	"	7.613	

A.2 α-β ANNEALED ALLOY

TIME SECONDS	SHEAR STRESS $x10^{-3}$ psi	SHEAR STRAIN $x10^{3}$	REMARKS
	4.747	0.676	No Creep
	9.945	1.33	No Creep
	14.242	2.116	No Creep
0	18.990	2.836	
13260	"	2.880	
24720	"	2.945	
78720	"	2.945	
0	21.363	3.250	
5300	"	3.272	
17030	"	3.294	
29618	"	"	
85838	"	"	
0	35.606	5.300	
6320	"	5.497	
20540	"	5.519	
57610	"	"	
0	47.474	7.024	
3120	"	7.264	
17970	"	7.330	
28210	"	7.352	
86710	"	7.374	
0	59.343	9.100	
11530	"	9.250	
19710	"	"	
23270	"	9.272	
108770	"	9.293	
0	71.211	11.191	
1740	"	12.631	
2940	"	13.045	
24240	"	17.081	

A.2 Continued

TIME SECONDS	SHEAR STRESS $x10^{-3}$ psi	SHEAR STRAIN $x10^{3}$	REMARKS
63500	71.211		
93450	"	26.505	
134780	"	29.363	
153300	"	30.563	
163530	"	31.152	
	59.343	29.385	
	47.474	27.574	
	35.606	25.785	
	23.737	23.866	
	14.242	22.382	
	4.745	20.790	
	0	19.961	

A.3 RECRYSTALLIZATION ANNEALED ALLOY

TIME SECONDS	SHEAR STRESS $x10^{-3}$ psi	SHEAR STRAIN $x10^{3}$	REMARKS
-	4.7474	0.676	No Creep
-	9.4948	1.309	No Creep
-	14.2422	2.094	No Creep
0	18.9896	2.771	
19620	"	2.901	
59300	"	"	
0	23.7370	2.600	
6690	"	3.665	
27400	"	3.709	
85850	"	3.730	
	35.606	5.476	
4060	"	5.585	
8100	"	5.607	
19320	"	5.628	
83500	"	"	
	47.474	7.374	
320	"	7.461	
34730	"	7.613	
73180	"	7.635	
	59.343	9.468	
3500	"	9.708	
41280	"	9.926	
80000	"	9.991	
89160	"	10.013	
	71.211	11.955	
100	"	12.784	
2000	"	15.096	
5100		17.016	
8460	"	17.539	

A.3 Continued

TIME SECONDS	SHEAR STRESS $x10^{-3}$ psi	SHEAR STRAIN $x10^{3}$	REMARKS
13530	71.211	20.724	
18540	"	22.470	
20630	"	23.080	
3272	"	26.091	
37300	"	27.051	
77970	"	32.548	
87690	"	33.486	
109560	"	35.188	
112260	"	35.449	
164710	"	38.351	
183520	"	39.223	
189260	"	39.442	
	59.343	37.805	
	47.474	35.908	
	35.606	34.053	
	23.737	32.199	
	18.990	31.501	
	14.242	30.716	
	9.495	29.952	
	4.747	29.123	
	0	28.272	
After 24 hrs	"	28.185	Creep Recovery

A.4 SOLUTION TREATED AT 900°C (1650°F) FOR 10 MIN + WATER QUENCH

TIME SECONDS	SHEAR STRESS $x10^{-3}$ psi	SHEAR STRAIN $x10^{3}$	REMARKS
	4.747	0.633	No Creep
	9.495	1.396	No Creep
	14.242	2.203	No Creep
	18.990	3.054	No Creep
0	23.737	3.905	
13360	"	"	
28082	"	3.927	
79415	"	"	
93626	"	3.949	
106040	"	"	
176040	"	"	
	"	"	
0	28.484	4.647	
3965	"	"	
89570	"	4.712	
138168	"	"	
158120	"	"	
0	35.606	5.890	
1030	"	5.912	
2503	"	5.955	
4293	"	5.977	
6448	"	"	
19450	"	5.999	
71039	"	6.043	
135600	"	6.065	
2600	"	"	

A.4 Continued

TIME SECONDS	SHEAR STRESS $x10^{-3}$ psi	SHEAR STRAIN $x10^{3}$	REMARKS
0	47.474	8.028	
960	"	8.115	
1930	"	8.137	
5990	"	8.202	
16300	"	8.224	
20630	"	"	
40390	"	"	
83720	"	8.246	
160990	"	"	
0	59.343	10.100	
50	"	10.602	
160	"	10.624	
1320	"	10.798	
2290	"	10.864	
5570	"	11.038	
10010	"	11.060	
13990	"	11.104	
18020	"	11.169	
23750	"	11.213	
29720	"	11.257	
76790	"	11.409	
80940	"	"	
106160	"	11.518	
153950	"	11.606	
236520	"	"	

A. 4 Continued

TIME SECONDS	SHEAR STRESS $x10^{-3}$ psi	SHEAR STRAIN $x10^{3}$	REMARKS
0	71.211	13.500	
50	"	15.576	
120	"	15.969	
220	"	16.361	
390	"	16.798	
630	"	17.234	
1000	"	17.670	
1200	"	17.867	
1400	"	17.997	
1500	"	18.085	
1600	"	18.172	
1800	"	18.303	
1950	"	18.390	
2200	"	18.499	
2515	"	18.674	
2840	"	18.826	
3000	"	18.914	
3380	"	19.154	
6000	"	19.874	
7230	"	20.201	
9490	"	20.615	
11570	"	20.877	
13830	"	21.139	
88780	"	24.302	
101500	"	24.673	
169970	"	25.545	
226450	"	26.243	
237200	"	"	
247940	"	26.309	

A.4 Continued

TIME SECONDS	SHEAR STRESS $x10^{-3}$ psi	SHEAR STRAIN $x10^{3}$	REMARKS
253750	71.211	26.374	
312570	"	26.745	
334760	"	26.898	
398370	"	27.203	
423780	"	27.291	
488700	"	27.531	
501730	"	27.618	
562300	"	27.836	
591050	"	27.901	
655330	"	28.181	
711340	"	28.338	
779060	"	28.512	
832140	"	28.774	
903450	"	28.839	
988920	"	29.014	
1077460	"	29.145	
1414930	"	29.668	
1497230	"	29.799	
1573940	"	29.843	
1632000	"	29.952	
1858270	"	30.192	
1944670	"	30.301	
2042560	"	30.345	
2123750	"	30.497	
2205170	"	30.541	
2322770	"	30.694	
2471000	"	30.846	
2559460	"	"	
2646840	"	30.977	
2749360	"	"	
2816440	"	"	

A.4 Continued

UNLOAD

TIME SECONDS	SHEAR STRESS $x10^{-3}$ psi	SHEAR STRAIN $x10^{3}$	REMARKS
0	59.343	29.319	
0	47.474	27.269	
0	35.606	25.153	
0	23.737	23.037	
0	14.242	21.117	
0	4.747	19.263	
0	0	18.325	
After 67 hrs	0	18.107	Creep Recovery

MICROSTRUCTURE OF SOLUTION TREATED AND QUENCHED Ti-6Aℓ-4V

ABSTRACT

The microstructure of solution treated and quenched Ti-6Aℓ-4V is reported with particular emphasis on the solution temperature of 900°C (1650°F). The alloy solution treated at 900°C was found to have a matrix of retained β mixed with martensite (α' or α"), within the matrix was primary α. Cyclic deformation of this alloy resulted in a transformation of the retained β to martensite (α' or α"). We propose that it is the strain induced transformation of retained β to martensite that is producing the improved fatigue life of this alloy. The microstructure of the alloy solution treated at 1065°C (1950°F) was totally martensite (α'), thus no retained β is present to transform upon cycling. The analysis of the alloy solution treated at 843°C (1550°F) is incomplete, but microstructural and microchemical analysis indicates that this alloy is composed of a β phase that is vanadium rich and primary α. The β phase is apparently stable when subject to cyclic deformation because of the high vanadium content. Lattice parameters and microchemistries of some of the phases are reported.

INTRODUCTION

In previous work we have observed that the fatigue life of Ti-6Aℓ-4V alloys is considerably increased by solution treatments of about 900° C. (1650° F.) followed by a water quench[1]. Annealed microstructures were observed to have an order of magnitude less fatigue life and solution temperatures of 55° C. higher of lower than 900° C. were shown to result in fatigue lives that are only one quarter of those solution treated at 900° C, this is shown in Table 1.

To understand why the solution treatment at 900° C. produced an increased fatigue life a detailed understanding of the Ti-6Aℓ-4V solution treated microstructure is necessary. In the experiments on fatigue life the results from the solution treated specimens were compared with results from specimens given an anneal in the $\alpha + \beta$ region; a similar comparison of microstructures will be made.

It is well accepted that the microstructure shown in figure 1, of the Ti-6Aℓ-4V alloy annealed in the $\alpha + \beta$ phase field has a matrix of hexagonal close packed (α) with the body centered cubic (β) forming in the grain boundaries. The microstructure of the solution treated Ti-6Aℓ-4V is not as well established although there has been some work directed at determining these microstructures. Williams and Blackburn[2] studied the phases present after quenching a Ti-6Aℓ-4V alloy from various solution temperatures. No quantitative

analysis was given for the phases present, but a qualitative analysis is presented. Williams and Blackburn defined the following phase fields for the following solution temperatures:

1000° C. (1832° F.) to 1100° C. (1922° F.) - $\alpha' + \beta$.

930° C. (1706° F.) to 1000° C. (1832° F.) - $\alpha' + \beta$.

900° C. (1652° F.) to 930° C. (1706° F.) - $\alpha' + \alpha'' + \beta + \alpha$.

860° C. (1580° F.) to 900° C. (1652° F.) - $\alpha' + \alpha$.

830° C. (1526° F.) to 860° C. (1580° F.) - $\alpha' + \beta + \alpha$.

RT to 830° C. (1526° F.) - $\alpha + \beta$.

In this presentation α' is the hexagonal martensite, and α'' is the orthorhombic martensite, the results of Williams and Blackburn here listed have been revised to the present convention and known structures. Fopiano, Bever and Averbach[3] have studied the phases present in solution treated Ti-6Aℓ-4V with x-ray diffraction. The phases they observed are listed with the solution temperatures:

1000° C. (1832° F.) - α' (Martensite)

950° C. (1742° F.) - $\alpha' + \alpha$ (Primary Alpha)

900° C. (1652° F.) - $\alpha' + \alpha$

850° C. (1562° F.) - $\alpha' + \alpha$

800° C. (1472° F.) - $\alpha' + \alpha$

These results are obviously quite different from those of Williams and Blackburn where retained β was found at nearly every temperature except for 860° C. to 900° C. However, Williams and Blackburn do not report the quantity of β so

we don't know the magnitude of the differences involved here. Earlier work by Griest, Doig and Frost[4] using x-ray diffraction techniques also reported only α and α' martensite for a solution temperature of 871° C. (1600° F.). Thus all of the authors appear to agree that in the solution temperature range 860° C. (1580° F.) to 900° C. (1652° F.) no β phase was observed, but at other temperatures Williams and Blackburn using transmission electron microscopy observed the presence of β. Only Fopiano et al. present any quantitative data as to the percentage of phases present, but their results are in disagreement with those of Williams and Blackburn. Thus it does appear that additional work is needed on verifying the phases present and quantifying their amounts, structure and composition. This will be a report on our progress to date on this work. In addition we will study the microstructures after cyclic deformation to monitor the changes resulting from fatigue damage. We will use a combination of transmission and scanning electron microscopy, x-ray and electron diffraction, and microprobe analysis. Our primary interest will be to characterize the alloy solution treated at 900° C. (1650° F.) for this is the solution temperature for which we have observed particularly large fatigue lives.

EXPERIMENTAL PROCEDURE

The material for this study was nominally Ti-6Aℓ-4V, 1.25 inch extruded rod of the composition in weight percent:

Aℓ	V	O	Fe	N	C	H
6.3	4.2	.188	.17	010	.02	67 ppm

The alloy was mill annealed, after extrusion, for 2 hours at 1300° F. The nominal tensile properties of the as received rod are:

Ultimate tensile strength - 147-157 ksi

Yield strength - 134-138 ksi

Elongation - 15 percent

Reduction in area - 32-39%

Rockwell "C" hardness - 32 to 35 .

The annealed specimens were all heated in a vacuum of better than 10^{-5} torr for the prescribed annealing procedure. In this work only one annealing procedure will be reported:

Recrystallize Anneal

928° C. (1702° F.) for four hours, furnace cool (FC) to 760° C. (1400° F.) at 180° C./Hr., FC to 482° C. (900° F.) at 372° C./Hr.; air cool to room temperature.

The annealed microstructure is compared with solution treated and quenched microstructures. The specimens were solution treated in a vertical air furnace for 10 minutes and

then the specimens were dropped into a water bath. The specimen temperature was measured with a thermocouple in the furnace that contacted the specimen.

For electron microscopy, thin sections of metal were cut with a spark cutter. The metal sections were further thinned by electropolishing in a solution of 62.5% methanol, 31% butanol and 6.5% perchloric acid (70% strength) at 13.9 volts and -40° C.

RESULTS AND DISCUSSION

The microstructure of the alloy solution treated for 10 minutes at 900° C. (1650° F.) will be discussed first because this solution temperature is of primary interest, then the results of other solution temperatures will be compared to the 900° C. (1650° F.) results. The transmission electron micrograph in Figure 2 shows particles (islands) of primary α in a matrix that is a mixture of retained β and martensite, Figure 2 contains the electron diffraction pattern identifying the phases as α' (hexagonal close packed), and β (body centered cubic). The lattice parameters of the α' and β are presented in Table 2. The lattice parameter data is necessary for phase identification. The martensite is indexed on a hexagonal Bravias lattice (α'); however, it is possible that the martensite is orthorhombic (α''). To the present time we have been unable to unambiguously characterize the martensite because of the similarity of the α' and α''. The orthorhombic Bravias lattice is obtained by a distorsion of the hexagonal cell such that the 6 fold symmetry of the basal plane is destroyed and the a and b axis of the orthorhombic

cell must be utilized rather than the a axis of the hexagonal. The distorsion is difficult to detect unless it is large, but it only requires a small distorsion to cause the structure to have an orthorhombic Bravias lattice, thus making unambiguous identification difficult. In the transmission electron micrograph of Figure 2 it is obvious that some acicular martensite has been formed, but it has proved difficult to obtain a diffraction pattern just from an acicular martensite grain because of its small size. Some diffraction spots from the acicular martensite have been observed mixed with those of the β phase, and the dark field image in Figure 3 is an indication of the morphology of the acicular martensite. The observation that the matrix is primarily retained β in the alloy solution treated at 900° C. and water quenched is at variance with the results of both Williams et al. and Fopiano et al., they observed α and martensite although Williams et al. leave open the possibility of a small amount of β. The explanation of this difference is not clear, but we are quite certain of our conclusion; to support our conclusion subsequent deformation of the alloy produces a martensitic transformation as will be discussed next. Only the metastable retained β could transform to martensite.

The microchemistry of the alloy solution treated at 900° C. (1650° F.) is given in Table 3. Our results are compared with the results presented by Fopiano et al. for a solution temperature of 900° C. The data of Fopiano et al. is not an experimental result, but rather it is based upon an analysis of previous phase diagram work. The results for vanadium are in

good agreement with our experiments, but the results for aluminum are in disagreement. In this work the α phase was found to be lower in Aℓ than predicted by Fopiano's analysis.

Our interest in studying the Ti-6Aℓ-4V alloy in the 900° C. solution treated condition is the observation of an improved fatigue life for this treatment. To understand the reason for the improved fatigue life we are studying the microstructure of this alloy before and after cyclic loading. A specimen of this alloy was subjected to cyclic deformation of $\sigma_{ALT} = \pm 5.4 \times 10^8$ N/M^2 (78 ksi) with R = - 0.3 for 1 X 10^6 cycles. Note in Figure 4 the increase in the percentage of martensite needles after the cyclic deformation in comparison to Figure 2. It appears that the cyclic deformation is inducing a β to martensite transformation. Further work is necessary to confirm the character of the transformation, but the initial transmission electron micrographs indicate that this is a martensite transformation.

The analysis of the alloy solution treated at 1066° C. (1950° F.) was quite simple. The structure was a α' martensite shown in Figure 5 with the lattice parameter shown in Table 2 obtained from the diffraction pattern. No microchemical analysis was performed on this alloy because it should all be of uniform composition. It is possible that small amounts of retained β could exist in this alloy, but none were detected.

The analysis of the alloy solution treated at 843° C. (1550° F.) is not yet complete; however, initial work indicates that the microstructure shown in Figure 6 is composed of primary alpha and retained β. These results are again at variance with

Fopiano et al.; however, Williams and Blackburn indicate that between 830°C. and 860° C. there is a mixture of $\alpha' + \beta + \alpha$; and that below 830° C. there is primary α and retained β. Our results are basically in agreement with Williams and Blackburn because we observe primary α and β, it is possible that there is a small amount of α' in addition that we have not been able to detect.

CONCLUSIONS

Our microstructure analysis is not as yet complete, but still the present results provide an indication of the mechanism that is resulting in the improved fatigue lives for the specimens solution treated at 900° C. (1650° F.) and water quenched. The matrix of this alloy as quenched is mostly retained β with some acicular martensite. After cyclic loading it is observed that a large fraction of the retained β in the matrix has transformed to acicular martensite. The structure of the martensite formed during quenching and during cycling of the 900° C. solution treated alloy have not been determined, but there are indications that both are orthorhombic[5]. It appears that the cyclic deformation is producing the martensitic transformation rather than fatigue damage. We propose that this might be a contributing factor to the increased fatigue life of this alloy, martensite is formed rather than fatigue damage.

The reason that this same mechanism does not work in the alloys given the other treatments is explained by our microstructural analysis. The alloy solution treated at 1066° C. (1950° F.) is fully transformed to martensite (α'), thus in this alloy there is no significant amount of retained β to transform.

The alloy solution treated at 843° C. (1550° F.) does not have as large a fatigue life as that solution treated at

900° C. (1650° F.) because the β phase is richer in vanadium at the lower solution temperature, this is shown in Table 3. where at 900° C. our results and those of Fopiano et al.[3] agree that there is about 6.6% vanadium in the β phase, but at the lower temperature of 850° C. the β phase has about 9% vanadium. The increased vanadium concentration tends to stabilize the β phase so that the β to martensite transformation has less probability of occurring. In the case of the recrystallize anneal alloy the β phase is stabilized during the slow cooling so that the β phase becomes rich in vanadium.

There is one possible explanation for the improved fatigue life that we have not separated from the explanation that is proposed above. That is that it is the presence of the finely dispersed martensite (probably orthorhombic α") shown in Figure 3 that is resulting in the improved fatigue life. Since the β in this microstructure also transforms to martensite during the cyclic deformation we have not been able to determine the relative effect of the transformation and the microstructure in which it occurs.

REFERENCES

1. M. A. Imam and C. M. Gilmore, Fatigue Life in Annealed and Martensitic Ti-6Aℓ-4V, Report IIb, Contract No. N00019-75-C-0093, August 1975.

2. J. C. Williams and M. J. Blackburn, Trans. ASM, 60 (1967) 373.

3. P. J. Fopiano, M. B. Bever, and B. L. Averbach, Trans. ASM, 62, (1969) 324.

4. A. J. Griest, J. R. Doig, and P. D. Frost, TMS - AIME 215 (1959) 627.

5. J. C. Williams, Titanium Science and Technology Eds. Jaffee and Burke, Plenum Press, New York, (1973) 1443.

Table 1

FATIGUE LIVES OF HEAT TREATED Ti-6Aℓ-4V ALLOYS CYCLED AT A SHEAR STRAIN OF ±0.02 PLUS AN AXIAL STRESS OF 2.12×10^7 N/M^2

HEAT TREATMENT*	MEAN**	MINIMUM	STANDARD DEVIATION
α-β ANNEAL	944	429	443
843°C (1550°F)ST + WQ	2497	1837	717
900°C (1650°F)ST + WQ	9616	8917	758
1065°C (1950°F)ST + WQ	2396	1633	487

* ST-solution treatment for 10 minutes
WQ-Water Quenched

** Results based upon four specimens for each heat treatment.

α-β Anneal - 800°C (1472°F) for 3 hours, furnace cool to 600°C (1112°F) Air cool to room temperature.

Table 2. Lattice Parameters of Ti-6Al-4V Phases

Heat Treatment[1]	Phase	Lattice Parameters in A°	Technique
R. A.	α	a = 2.924 c = 4.671	X-R-D
R. A.	α	a = 2.925 c = 4.670	E-D
1066 C. - ST + WQ	α'	a = 2.921 c = 4.663	X-R-D
1066 C. - ST + WQ	α'	a = 2.925 c = 4.634	E-D
900 C. - ST + WQ	α	a = 2.942 c = 4.738	E-D
900 C. - ST + WQ	α'	a = 2.931 c = 4.696	E-D
900 C. - ST + WQ	β	a = 3.299	

1. R. A. : Recrystallize Anneal

   ST: Solution treated for 10 min.

   WQ: Water quench

2. X-R-D: X-ray diffraction

   E-D: Electron diffraction

Table 3. Microchemistry of Ti-6Aℓ-4V Solution Treated and Quenched

Solution Temperature	Phases Observed	Phase Composition		Reference
		Aℓ	V. Wt %	
900° C.	α	7.49 ± .1	2.51 ± .12	This
(1650 ° F.)	α' + β	5.8 ± .26	6.66 ± .65	Work
900° C.	α	9	2.5	3
	α'	2	3.5	
850° C.	α	8	2.5	3
	α'	2	8	

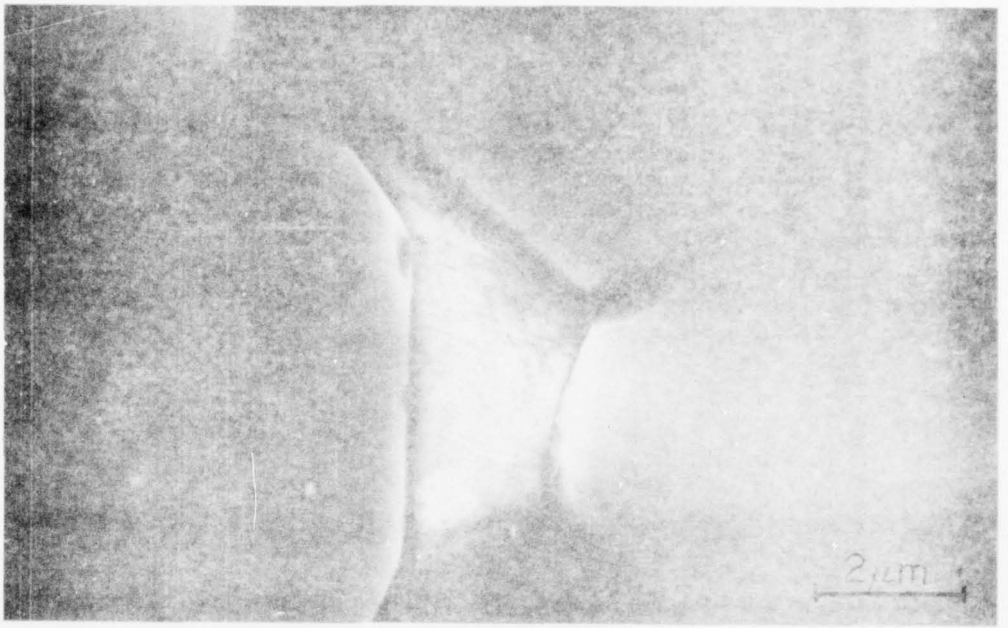

Figure 1 Transmission electron micrograph (TEM) of the recrystallize anneal microstructure showing the primary α and the grain boundary β.

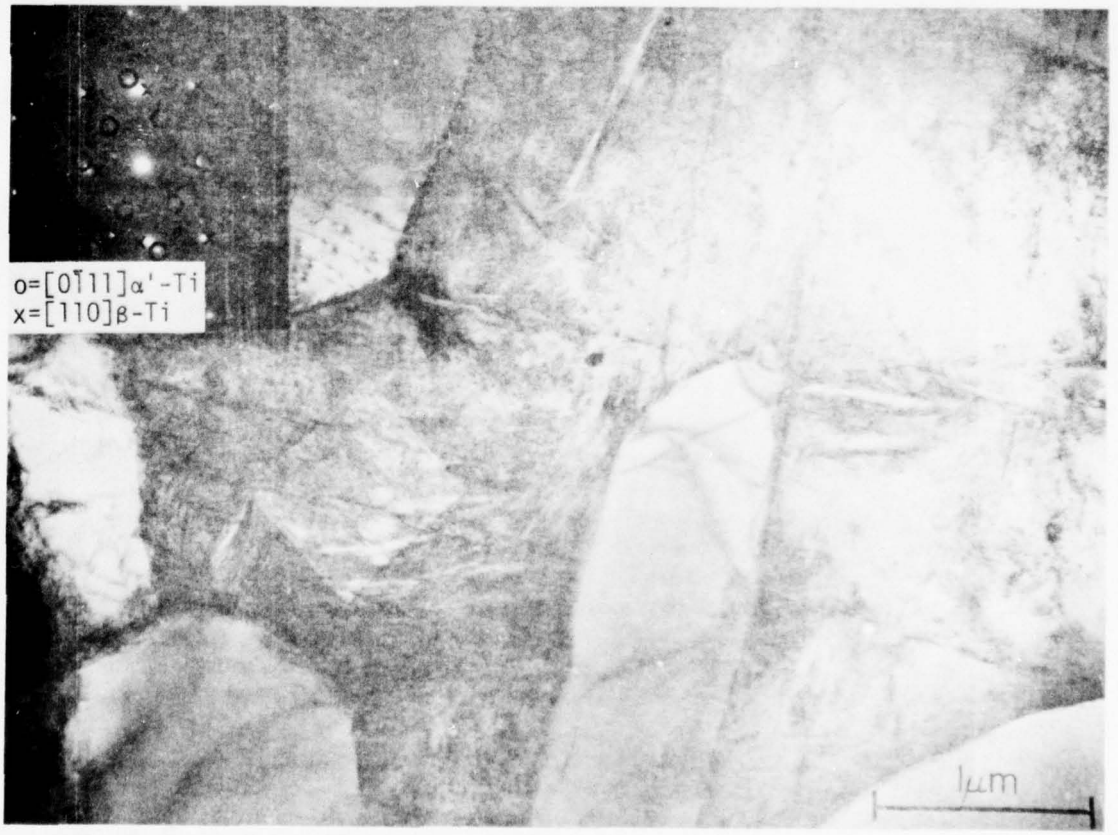

Figure 2 TEM of the alloy solution treated at 900° C. (1650°F.) for 10 min. and water quenched. The diffraction pattern taken from the matrix of the alloy indexes as a mixture of α' (martensite) and retained β. The light areas are primary α.

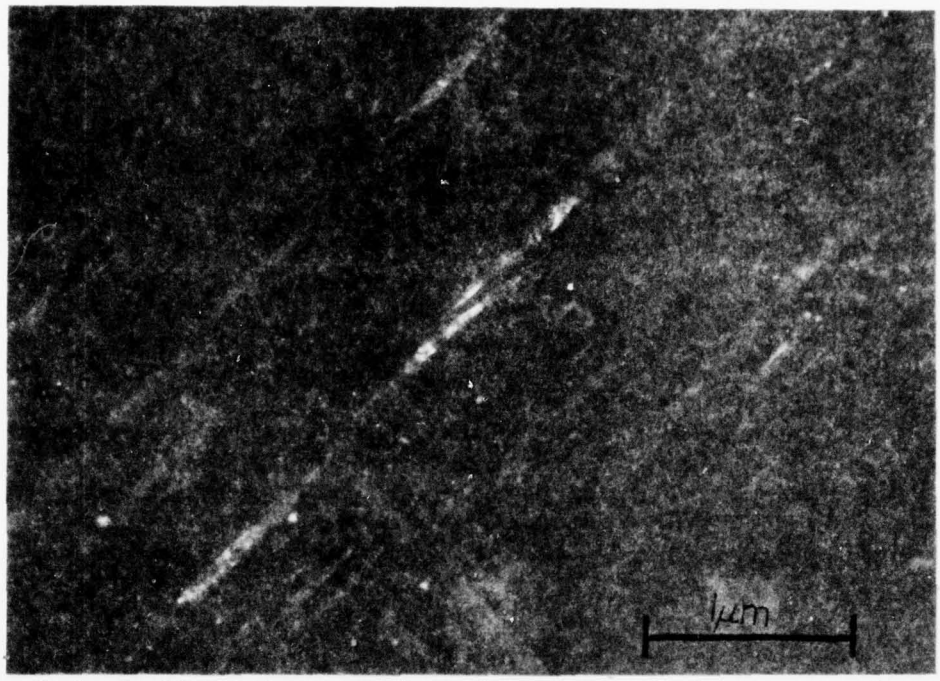

Figure 3 A dark field image taken from one of the martensite reflections in Figure 2, this shows the morphology of the martensite.

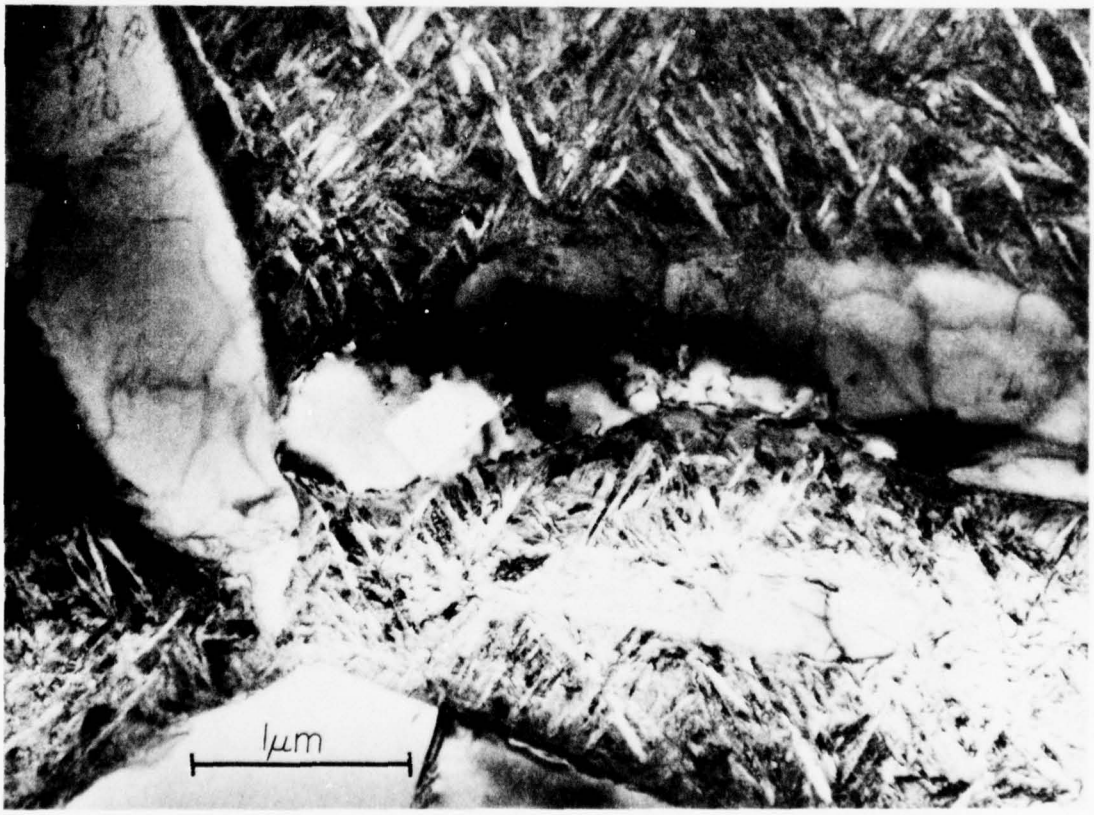

Figure 4 TEM from the same alloy shown in Figure 2 after 10^6 fatigue cycles of σ_{ALT} = 78 ksi with R=-0.3 in tension.

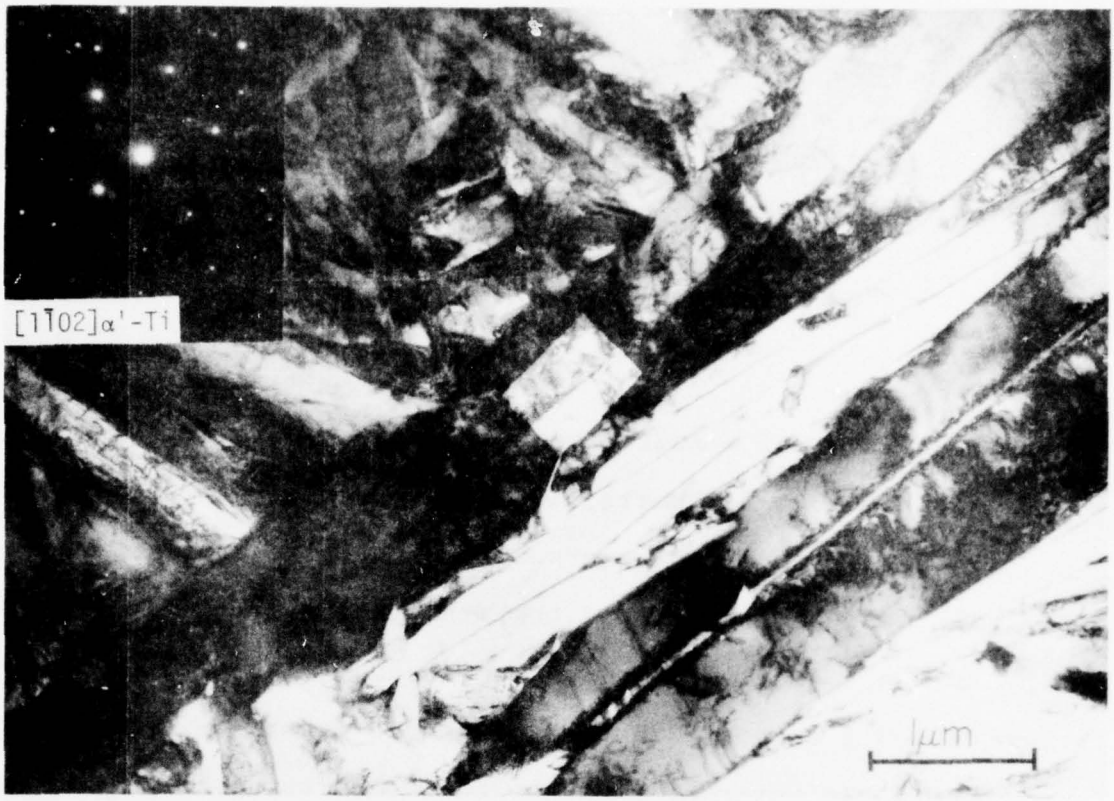

Figure 5 TEM of the alloy solution treated at 1066° C. (1950° F.) for 10 min. and water quenched. The electron diffraction pattern indexes to be α' (hexagonal) martensite.

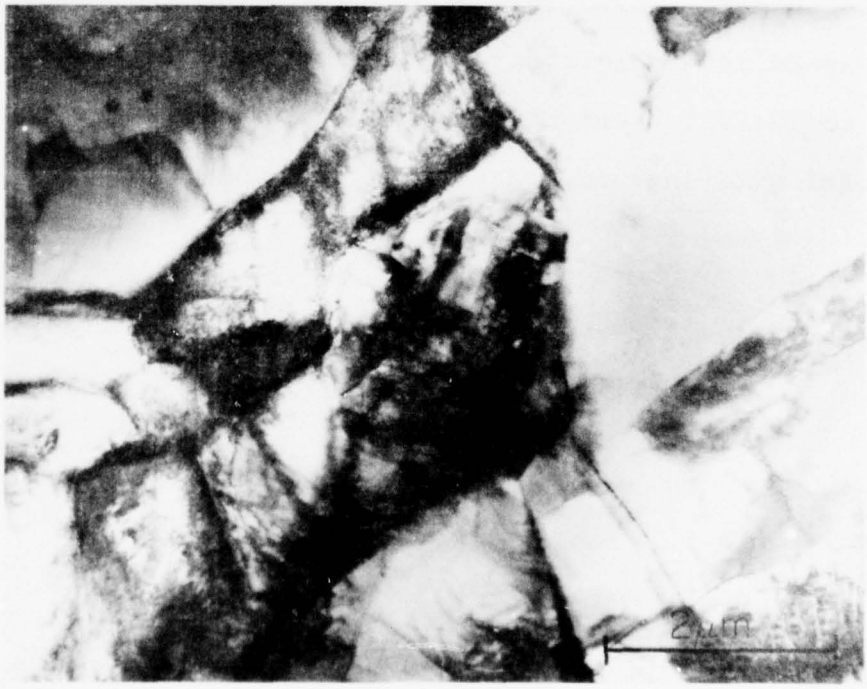

Figure 6 TEM from the alloy solution treated at 843° C. (1550° F.) for 10 min. and water quenched.

A STUDY OF FATIGUE DAMAGE WITH ULTRASONIC INTERNAL FRICTION MEASUREMENTS

ABSTRACT

Internal friction measurements using a resonance technique at kilohertz (17650 Hz) frequency were made on Ti-6Aℓ-4V that had been subject to cyclic fatigue loading. The measurements showed that the internal friction increased as the fatigue damage was increased. Also fatigue damage caused a decrease in the ultrasonic strain wave amplitude where the internal friction becomes strongly amplitude dependent, ie where the ultrasonic wave began to fatigue the specimen. These initial results indicate that the ultrasonic internal friction at kilohertz frequencies is sensitive to initial fatigue damage and it may be an effective tool for studying and monitoring fatigue damage.

A STUDY OF FATIGUE DAMAGE WITH ULTRASONIC INTERNAL FRICTION MEASUREMENTS

INTRODUCTION

There have been some past attempts at studying fatigue damage with measurements of internal friction. One commonly employed technique is the measurement of the attenuation of an ultrasonic wave using a pulse-echo type measuring system. However, the results from these experiments are quite contradictory. For example Joshi and Green[1] used a pulse-echo method to study fatigue in aluminum and steel. In both cases they found that the ultrasonic attenuation was nearly constant during fatigue testing until about 70% (steel) to 80% (aluminum) of the specimen life was consumed, then an increase in ultrasonic attenuation was observed and just before final fracture the ultrasonic attenuation increased drastically. No correlation between the ultrasonic attenuation and the fatigue damage is presented by Joshi and Green, but it is most likely that the ultrasonic wave was attenuated by the presence of the crack. This technique appeared to be insensitive to the initial cycles before crack initiation, thus the technique does not appear to be sensitive to the accumulation of fatigue damage before the crack initiation stage. A similar technique was utilized by Bratina and Mills[2] to study fatigue damage in 4340 steel, but the results are quite different. Bratina and Mills observed that in slow

cycling (1 Hz) of 4340 steel the internal friction continually decreased with cyclic straining, this they attributed to strain aging. Bratina and Mills correlated their results with dislocation behaviour but no correlation was made with microscopic fatigue damage. Thus the results of Joshi and Green are quite different than the results of Bratina and Mills. There also has been interest in using the exponential decay of a pulse to determine the internal friction. Several Soviet publications deal with this technique; for example Shevelya and Otblesk[3] used the decay of oscillations to determine the internal friction in copper and steel during fatigue. In copper they found that the internal friction first increased with cycling, they attribute this to an initial increase in dislocation density and length. Then they observed that the internal friction reached a peak at about 10% of the life and began to decrease. They attribute the decrease in internal friction to a shortening of the dislocation loops due to pinning by point defects. The internal friction continued to decrease until a minimum value was observed at the time of crack initiation. After crack initiation the internal friction increased rapidly until failure occurred. The response from steel was somewhat different; several maximums and minimums were observed in the internal friction as the fatigue damage increased, also in copper high amplitudes of stress produced smaller changes in internal friction than low amplitudes, whereas in steel higher amplitudes of stress produced larger changes in the magnitude of internal friction.

Again, no correlation was made between these measurements of internal friction and the microstructural changes. This technique does appear to be sensitive to microstructural changes before and after crack initiation, and thus has an advantage over the ultrasonic method at megahertz frequencies.

Mason[4] has developed a technique for studying the internal friction of metals using ultrasonic waves of kilohertz frequency. The unique feature of this technique is that the ultrasonic wave amplitude can be varied so that ultrasonic waves of longitudinal strain amplitude from 10^{-6} in/in to 10^{-2} in/in can be produced in the specimen. Since the internal friction can be amplitude dependent this variable amplitude adds considerable versatility to this technique. It is possible to increase the strain wave amplitude to where the ultrasonic waves begin to fatigue the specimen. When the specimen begins to fatigue the internal friction begins to increase sharply. Mason and MacDonald[5] used this technique to fatigue a specimen of Ti-6Aℓ-4V at ultrasonic frequency. After fatiguing the specimen at ultrasonic frequency they observed that upon retesting the specimen, the sharp increase in internal friction that indicates fatigue occurred at an ultrasonic strain wave amplitude nearly an order of magnitude smaller than before fatigue. Also they observed that the base line value of the internal friction had increased nearly an order of magnitude after the ultrasonic fatigue. Mason and Wood[6] have correlated the

changes in microstructure with the observed changes in internal friction for metals like copper and iron. They found that the formation of persistent slip bands corresponded with the sharp increase in internal friction. However, the fatigue damage due to ultrasonic kilocycles was much different than that of low frequency testing. They observed at the high frequencies only a few very narrow isolated slip bands had formed, where as, at low frequency the persistent slip bands would spread throughout the specimen. Despite there being only a few isolated spots of fatigue damage there were very large changes in the internal friction. Thus it appears that the energy absorbed out of the ultrasonic strain wave is selectively absorbed at these localized persistent slip bands, unless some unobserved change is occurring in the bulk of the specimen. Because of the apparent selectivity of this ultrasonic technique for absorbing energy at fatigue damaged areas it might be possible to use this ultrasonic internal friction technique to study the accumulation of fatigue damage that occurs at more conventional frequencies. In this research we will use the techniques developed by Mason to study specimens that have been subjected to fatigue damage.

EXPERIMENTAL PROCEDURE

The system used for the measurement of the internal friction is shown in Figure 1. It consists of a PZT 4 ceramic driver cemented to a mechanical transformer with epoxy resin which can withstand large strains. The mechanical transformer has diameters of 1.75 in. and 0.35 in. resulting in a diameter ratio of 5 to 1; this results in a displacement ratio of 25 to 1.

It has been shown that the internal friction (Q^{-1}), and the longitudinal strain applied to the specimen (S_{11}), both can be determined by measuring the voltage applied (V_a) to the transducer, the pickup voltage (V_{pu}) from electrodes mounted at the center of the transducer and the resonant frequency of the system. Calibration of this system has shown that the longitudinal strain is given by the following equation:

$$S_{11} = (7)(1.65\text{x}10^{-5})\ V_{pu} = 1.155\text{x}10^{-4}\ V_{pu} \qquad (1)$$

and the internal friction (Q^{-1}) is given by:

$$Q^{-1} = 1.326\text{x}10^{-3}\ \left(\frac{V_a}{V_{pu}} - 0.168\right) \qquad (2)$$

The details of measuring the parameters for these equations is discussed by Mason[4].

The specimen must be made to resonate at the system frequency which is about 17,650 Hz, the dimensions shown in Figure 2 resulted in the proper resonant frequency for the Ti-6Aℓ-4V used in this experiment. The actual chemical

composition for this alloy was in wt. percent:

Aℓ	V	O	Fe	N	C	H
6.3	4.2	.188	.17	.010	.02	67ppM

The mill annealed material for these specimens was machined on a lathe to the dimensions shown except that about 0.020 inches of extra metal was provided in the necked down portion. The specimens were then annealed in a vacuum better than 10^{-5} torr at 500°C for four (4) hours and furnace cooled. They were then polished to the final dimensions with a 0.1 micron surface.

The specimen is tuned to the resonant frequency by polishing in down to the proper dimension, a typical specimen and dimensions is shown in Figure 2. The tuning is controlled by the equation:

$$\tan \frac{\omega l_1}{v_1} = \left(\frac{Z_{02}}{Z_{01}}\right)^{\frac{1}{2}} \qquad (3)$$

Where ω is the resonant frequency, l_1 is the specimen length, v_1 is the velocity of sound, Z_{01} and Z_{02} are the impedance of the large and small sections of the specimen. The ratio of the impedances Z_{02}/Z_{01} can be taken as the ratio of the masses of the large and small sections for this calculation. The specimen must be closely tuned to the resonant frequency otherwise the output from the oscillator decreases sharply, this is demonstrated in Figure 3 where the resonant frequency of the system with a specimen attached is plotted as a function of the output voltage (V_{pu}). The resonant frequency of the system alone is about 17650 Hz, as can be seen from

Figure 3 when the resonant frequency of system with a specimen attached approaches the resonant frequency of the driver alone the maximum output is observed. In this experiment the resonant frequency of a specimen could be changed by changing Z_{02} in equation 3, this is done by polishing off some material thereby reducing Z_{02} thus changing ω to satisfy equation 3.

After the specimen is tuned and polished the internal friction is determined as a function of the ultrasonic strain wave amplitude, a typical result for the initial unfatigued material is shown in Figure 4. The internal friction is observed to be relatively independent of the ultrasonic strain wave amplitude until the wave produces strains of 4×10^{-4} then the internal friction becomes strongly amplitude dependent. It has been observed that the amplitude dependent section corresponds to movement of dislocations and that the specimen fatigues if the ultrasonic strain wave amplitude is further increased. In these studies the ultrasonic strain wave amplitude was increased until the amplitude dependent region was observed, and the test was terminated below the strains that would produce additional fatigue.

The specimen shown in Figure 2 was then subjected to fully reversed fatigue straining (R=-1) for a fraction of the expected fatigue life. The internal friction was then again determined as a function of ultrasonic strain wave amplitude until the internal friction was observed to be amplitude dependent; then the internal friction test was terminated and more cycles were applied and the internal

friction redetermined. The results of such a sequence of tests are shown in Figure 4.

The fatigue cycling was performed at room temperature at a frequency of 0.2 Hz. The specimen shown in figure 2 was clamped in a special fixture designed to accommodate the large ends of the specimen. The fatigue machine produces a cyclic angular displacement which for the strains listed in figure 4 were 2.4° (0.009) and 3.19° (0.012). The strains were calculated by assuming that the strain in the specimen was localized over the straight portion of gage length of 0.426 (.676 - .250) in. There is of course some error in this assumption for some strain will occur in the curved portion of the specimen, but this refined calculation did not seem necessary for this presentation.

RESULTS AND DISCUSSION

In the results shown in Figure 4 the tests were started at a shear strain amplitude of ±0.009, after initiating the test it became apparent that it would require too much time to complete the test thus this amplitude was terminated after 1400 cycles. The shear strain amplitude was increased to ±0.012 and after 800 cycles of ±0.012 shear strain the internal friction was again determined. In Figure 4 it can be seen that this fatigue loading resulted in an increase in internal friction, also the internal friction became strongly amplitude dependent at a smaller strain (3×10^{-4}). The specimen was then fatigued for four hundred additional cycles. The internal friction was again determined as a function of strain amplitude, this data is also shown in Figure 4. Again the internal friction increased; however, no subsequent change was observed in the strain (S_{11}) where amplitude dependent internal friction was observed. Relative to the unstrained state, a 60% increase in internal friction was observed after the 1200 cycles at ±0.012. The specimen was again fatigued, but failure occurred after 1749 cycles and no measure of internal friction was made before the final fracture.

CONCLUSIONS

The tests shown in Figure 4 indicate that the value of the internal friction (Q^{-1}) is sensitive to fatigue cycling. Of particular interest is that the internal friction appears to increase continuously with cycling, thus the technique might allow a continuous monitoring of the condition of the metal during cyclic loading. This is a considerable advantage in comparison to the result of Joshi and Green where an increase in ultrasonic attenuation at megacycle frequency occurred just prior to final failure. More experiments need to be run to correlate the internal friction with the fraction of fatigue life, and to correlate the internal friction with microstructural changes.

In Figure 4 the internal friction of the annealed specimen becomes strongly amplitude independent at a longitudinal strain wave amplitude of 4.25×10^{-4}. Above this strain wave amplitude the specimen is being fatigued. After fatigue cycling for 800 cycles at ± 0.012 the internal friction becomes strongly amplitude dependent at a strain of 2.9×10^{-4}, thus the ultrasonic wave can fatigue the specimen at a lower strain amplitude. This indicates that the cyclic loading has weakened the material. Experimentally, it is very difficult to determine the point at which the specimen begins to become unstable during the ultrasonic internal friction measurement without permanently damaging the specimen. Thus in our future work we plan to

concentrate our effort on the change that occurs in the amplitude independent internal friction. This should allow us to apply this technique to larger specimens with lower amplitudes of strain wave that would be non damaging to the specimen.

REFERENCES

1. N. R. Joshi and R. E. Green, Engr. Fract. Mech., 4 (1972) 577-583.

2. W. J. Bratina and D. Mills, Canadian Met. Quart. 1 (1962) 83-97.

3. V. V. Shevelya and B. E. Otblesk, Fiziko-khimicheskaya Mekhanika Materialov, 8, 3 (1972) 257-261 (English translation), 7-12 (Russian).

4. W. P. Mason, Microplasticity ed. C. J. McMahon, Interscience (1968) 287-364.

5. W. P. Mason and D. E. MacDonald, J. Acoust. Soc. Am. 51 (1972) 894-899.

6. W. P. Mason and W. A. Wood, Jour. Appl. Phys., 39, 12 (1968) 5581-5584.

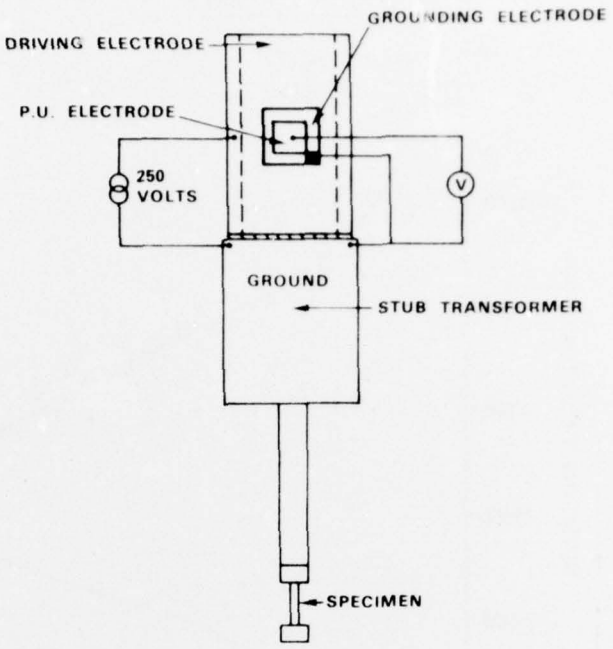

Figure 1 Schematic diagram of the ultrasonic driver. The driving electrode is a PZT-4 piezoelectric cylinder attached to a Ti-6Aℓ-4V stepped transformer. The specimen details are shown in Figure 2.

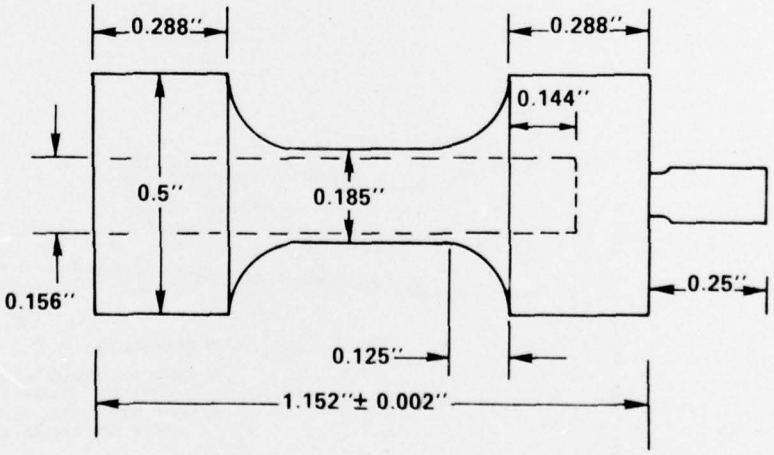

Figure 2 Dimensions for the Ti-6Aℓ-4V specimen used in this experiment. The curvature between the center and the ends was to localize the fatigue damage at the specimen center.

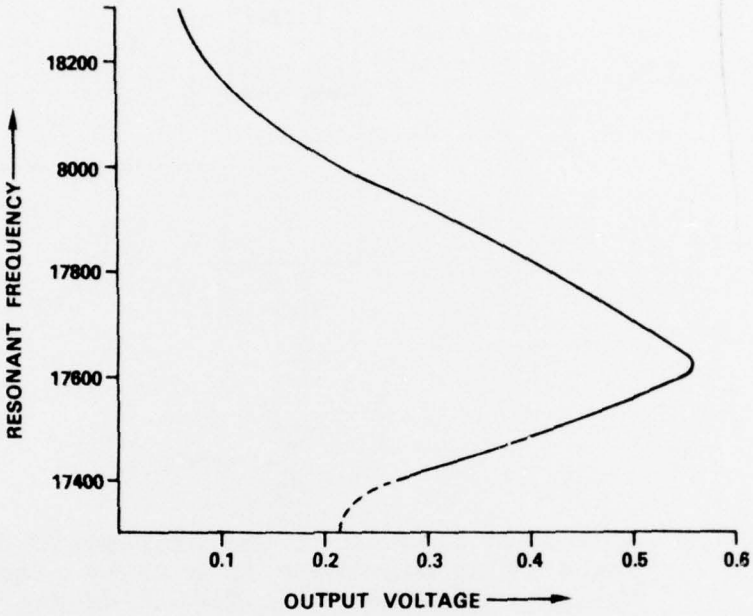

Figure 3 System output as a function of resonant frequency. When the system is tuned to about 17650 Hz maximum output is observed.

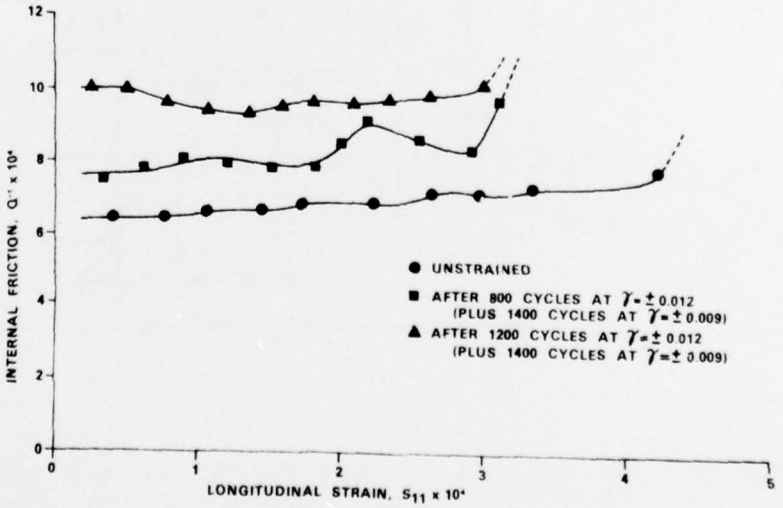

Figure 4 Internal friction as a function of the ultrasonic strain wave amplitude determined for an annealed unstrained specimen and after the fatigue cycles indicated.

Security Classification

DOCUMENT CONTROL DATA - R & D

(Security classification of title, body of abstract and indexing annotation must be entered when the overall report is classified)

1. ORIGINATING ACTIVITY (Corporate author)	2a. REPORT SECURITY CLASSIFICATION
Institute for Fatigue, Fracture and Structural Reliability The George Washington University	Unclassified 2b. GROUP

3. REPORT TITLE

A. Mechanical Properties of Annealed and Martensitic Ti-6Al-4V.
B. Microstructure of Solution Treated and Quenched Ti-6Al-4V.
C. A Study of Fatigue Damage with Ultrasonic Internal Friction Measurements.

4. DESCRIPTIVE NOTES (Type of report and inclusive dates)

Technical Report

5. AUTHOR(S) (First name, middle initial, last name)

C. M. Gilmore and M. A. Imam

6. REPORT DATE	7a. TOTAL NO. OF PAGES	7b. NO. OF REFS
August 1976	63	A(3), B(5), C(6)

8a. CONTRACT OR GRANT NO.	9a. ORIGINATOR'S REPORT NUMBER(S)
N00019-76-C-0136 b. PROJECT NO.	III
c. d.	9b. OTHER REPORT NO(S) (Any other numbers that may be assigned this report)

10. DISTRIBUTION STATEMENT

Approved for public release
Distribution unlimited

11. SUPPLEMENTARY NOTES	12. SPONSORING MILITARY ACTIVITY
	Naval Air Systems Command

13. ABSTRACT

A. Mechanical Properties of Annealed and Martensitic Ti-6Al-4V.

Fatigue life studies are reported on annealed microstructures and on solution treated plus quenched microstructures, and it was found that specimens solution treated at about 900°C (1650°F) had the longest fatigue life, longer by at least a factor of four. A comparison of the α-β annealed alloy with the alloy solution treated at 900°C (1650°F) demonstrated that increases in allowable strain of as much as 50% occurred at high strain amplitude. Annealing and elevated temperature testing appear to decrease the fatigue life of the as quenched alloy. Tensile tests of the alloy solution treated at 900°C showed that this treatment resulted in a high tensile strength and a high ductility (reduction in area) relative to commonly used anneal treatments. Room temperature static load creep tests showed that the alloy solution treated at 900°C had a high elastic limit and a relatively small amount of static creep.

B. Microstructure of Solution Treated and Quenched Ti-6Al4V.

The microstructure of solution treated and quenched Ti-6Al-4V is reported with particular emphasis on the solution temperature of 900°C (1650°F). The alloy solution treated at 900°C was found to have a matrix of retained β mixed with martensite (α' or α"), within the matrix was primary α. Cyclic deformation of this alloy resulted in a transformation of the retained β to martensite (α' or α"). We propose that it is the strain induced transformation of retained β to martensite that is producing the improved fatigue life of this alloy. The microstructure of the alloy solution treated at 1065°C (1950°F) was totally martensite (α') thus

DD FORM 1 NOV 65 1473 (PAGE 1)

S/N 0101-807-6801

Unclassified
Security Classification

14 KEY WORDS	LINK A		LINK B		LINK C	
	ROLE	WT	ROLE	WT	ROLE	WT

Abstract continued

no retained β is present to transform upon cycling. The analysis of the alloy solution treated at 843°C (1550°F) is incomplete, but microstructural and microchemical analysis indicates that this alloy is composed of a β phase that is vanadium rich and primary α. The β phase is apparently stable when subject to cyclic deformation because of the high vanadium content. Lattice parameters and microchemistries of some of the phases are reported.

C. A Study of Fatigue Damage with Ultrasonic Internal Friction Measurements.

Internal friction measurements using a resonance technique at kilohertz (17650 Hz) frequency were made on Ti-6Aℓ-4V that had been subject to cyclic fatigue loading. The measurements showed that the internal friction increased as the fatigue damage was increased. Also fatigue damage caused a decrease in the ultrasonic strain wave amplitude where the internal friction becomes strongly amplitude dependent, ie where the ultrasonic wave began to fatigue the specimen. These initial results indicate that the ultrasonic internal friction at kilohertz frequencies is sensitive to initial fatigue damage and it may be an effective tool for studying and monitoring fatigue damage.

KEY WORDS

Titanium alloys, fatigue, yield strength, tensile strength, elastic modulus, ductility, martensite, lattice parameters, microchemistry, solution treatment, internal friction.

DISTRIBUTION LIST

(One copy unless otherwise noted)

Naval Air Systems Command
Attn: Mr. M. D. Valentine
AIR-52031F
Washington, DC 20361
(1 copy plus balance after distribution)

Commander
Naval Air Development Center
(Code 302)
Warminster, PA 18974

Naval Ships Systems Command
(Code 03423)
Department of the Navy
Washington, DC 20360

Naval Ships Research & Development Center
(Code 2812)
Annapolis, MD 21402

Naval Ships Research & Development Center
Washington, DC 20007
attn: Mr. Abner R. Willner
Chief of Metals Research

Commander
Naval Ordnance Laboratory
(Metallurgy Division)
White Oak
Silver Spring, MD 20910

Director, Naval Research Laboratory
(Code 6320)
Washington, DC 20390

Office of Naval Research
The Metallurgy Program, Code 471
Arlington, VA 22217

Commander
Naval Air Systems Command Representative
Atlantic
Naval Air Station
Norfolk, VA 23511

Commander
Naval Air Systems Command Representative
Pacific
Naval Air Station, North Island
San Diego, CA 92135

Commanding Officer
Naval Air Rework Facility (Code 34100)
Naval Air Station
Alameda, CA 94501

Commanding Officer
Naval Air Rework Facility (Code 34100)
Marine Corps Air Station
Cherry Point, NC 28533

Commanding Officer
Naval Air Rework Facility (Code 34100)
Naval Air Station
Jacksonville, FL 32212

Commanding Officer
Naval Air Rework Facility (Code 34100)
Naval Air Station
Norfolk, VA 23511

Commanding Officer
Naval Air Rework Facility (Code 34100
Bldg. 604
Naval Air Station
Pensacola, FL 32508

Commanding Officer
Naval Air Rework Facility (Code 34100)
Naval Air Station, North Island
San Diego, CA 92135

Wright-Patterson Air Force Base
OH 45433
Attn: W. Griffith, AFML/LLS

Wright-Patterson Air Force Base
OH 45433
Attn: D.A. Shinn, AFM / MXA

Wright-Patterson Air Force Base
OH 45433
Attn: C.L. Harmsworth, AFML/MKE

Wright-Patterson Air Force Base
OH 45433
Attn: Dr. W. H. Reimann, AFML/LLM

Pittsburgh DCAS District
1610-S Federal Building
1000 Liberty Avenue
Pittsburgh, PA 15222
Attn: Z. D. Mosko

Army Materials & Mechanics Research Center
Watertown, MA 02172
Attn: Dr. A. Gorum

Commanding Officer
Office of Ordnance Research
Box CM, Duke Station
Durham, NC 27706

Commanding Officer
Corps of Engineers, U.S. Army
Coastal Engineering Research Center
5201 Little Falls Road, NW
Washington, DC 20016
Attn: Mr. R. Connolly, Librarian

Commanding Officer
Frankford Arsenal
Philadelphia, PA 19173
Attn: Mr. H. Markus, 1320 Bldg. 64-4

U.S. Army Tank & Automotive Command
28251 Van Dyke
Warren, MI 48090
Attn: Mr. Charles Green
Chief of Materials Laboratory

National Aeronautics & Space Administration
(Code RWM)
600 Indepedence Ave., SW
Washington, DC 20546

National Aeronautics & Space Administration
Langley Research Center
Materials Division, Langley Station
Hampton, VA 23365
Attn: Mr. H. F. Hardrath
Stop 188M

National Aeronautics & Space Administration
George C. Marshall Space Flight Center
Huntsville, AL 35812
Attn: Mr. J. G. Williamson
S&E-ASTN-MMC

National Academy of Sciences
Materials Advisory Board
Washington, DC 20418
Attn: Dr. J. Lane

U.S. Atomic Energy Commission
Document Library
Germantown, MD 21403

Director
National Bureau of Standards
Washington, DC 20234
Attn: Dr. E. Passaglia

Battelle Memorial Institute
Structural Materials Engineering
505 King Avenue
Columbus, OH 43201
Attn: Walter S. Hyler

Battelle Memorial Institute
505 King Avenue
Columbus, OH 43201
Attn: Mr. Stephan A. Rubin, Mgr.
Information Operations

IIT Research Institute
Metals Research Department
10 West 35th Street
Chicago, IL 60616
Attn: Dr. M. Parikh

Convair Aerospace
P.O. Box 80847
San Diego, CA 92138
Attn: Mr. Jack Christian, Code 64

Convair Division
General Dynamics
San Diego, CA 92112
Attn: Mr. A. Hurlich

Kaman Aerospace Corporation
Old Windsor Road
Bloomfield, CT 06001
Attn: Mr. M. L. White

Sikorsky Aircraft
Division of United Aircraft Corp.
Stratford, CT 06497
Attn: Dr. M. J. Salkind

Grumman Aerospace Corporation
Plant 12
Bethpage, NY 11714
Attn: R. Heitzmann

Grumman Aerospace Corporation
Plant 26, Research Department
Bethpage, NY 11714
Attn: Dr. Gary Goshwind

The Boeing Company
Material Technology Section
Wichita, KS 67210
Attn: Mr. Gayle Wadsworth

Lockheed-Georgia Company
Marietta, GA 30061
Attn: E. Bateh

The Boeing Company
Commerical Airplane
ORG 6-8733, MS77-18
P.O. Box 3707
Seattle, WA 98124
Attn: Cecil E. Parsons

The Boeing Company
Aerospace Division
P.O. Box 3707
Seattle, WA 98124
Attn: Mr. E. C. Bovee

Northrop Corporation
Aircraft Division
Dept. 3771-62
3901 West Broadway
Hawthorne, CA 90250
Attn: Mr. Allen Freedman

LTV Aerospace Corporation
Vought Aeronautics Division
P.O. Box 5907
Dallas, TX 75222
Attn: Mr. A. Hobran

Rockwell International
Columbus Division
Columbus, OH 43216
Attn: Mr. P. Maynard, Dept. 75
Group 521

Rockwell International
Rocketdyne Division
Canoga Park, CA 91305
Attn: Dr. Al Jacobs

Rockwell International
Los Angeles Division
International Airport
Los Angeles, CA 90008
Attn: Gary Keller
Materials Applications

Lockheed Palo Alto Research Laboratories
Materials Science Laboratory
3251 Hanover Street
Palo Alto, CA 94303
Attn: Dr. Frank A. Crossley
52-31/204

Lockheed California Company
P.O. Box 551
Burbank, CA 91503
Attn: Dr. J. Wooley
Mr. Virgil D. Moss, Unit 43
(two copies)

Lockheed Missile & Space Corporation
P.O. Box 501-ORGN 80-72
Bldg. 18
Sunnyvale, CA 91088
Attn: Dr. M. I. Jacobson

Lockheed Missile & Space Corporation
Box 504
Sunnyvale, CA 94088
Attn: Mr. G. P. Pinkerton
Bldg. 154, Dept. 8122

Douglas Aircraft Company
3855 Lakewood Boulevard
Long Beach, CA 90908
Attn: Mr. Fred Mehe, C1-250

McDonnell Aircraft Company
St. Louis, MO 63166
Attn: Mr. H. J. Siegel
Materials & Processes Dev. Dept.
General Engineering Division

McDonnell-Douglas Research Labs
St. Louis, MO 63166
Attn: Dr. D. P. Ames

Bell Aerosystems Company
Technical Library
P.O. Box 1
Buffalo, NY 14240

General Electric Company
Aircraft Engine Group
Materials & Processes Technology Labs.
Evendale, OH 45215

Solar
2200 Pacific Highway
San Diego, CA 92112
Attn: Dr. A. Metcalfe

Lycoming Division
AVCO Corporation
Stratford, CT 06497

General Electric Company
Corporate Research & Development
P.O. Box 8
Sehcnectady, NY 12301
Attn: D. Wood

Westinghouse Electric Company
Materials & Processing Laboratories
Beulah Road
Pittsburgh, PA 15235
Attn: Don E. Harrison

Dr. John D. Wood
Associate Professor
Lehigh University
Bethlehem, PA 18015

Goodyear Aerospace Corporation
Plant B, Dept. 690
Akron, OH 44315
Attn: A. G. Tokarcik

Mr. Jack D. Tree, Dept. 93-35-5M
AirResearch Manufacturing Co.of Arizona
Sky Harbor Airport
402 S. 36th Street
Phoenix, AZ 85034

Boeing-Vertol Company
Boeing Center
P.O. Box 16858
Philadelphia, PA 19142
Attn: Mr. J. M. Clark

Martin Marietta Aluminum Company
19200 Southwestern Avenue
Torrance, CA 90509
Attn: Mr. G. A. Moudry

TRW, Inc.
23555 Euclid Avenue
Cleveland, OH 44117
Attn: Elizabeth Barrett
T/M 3417

The Dow Metal Products Company
Hopkins Building
Midland, MI 48640

Detroit Diesel Allison Division
General Motors Corporation
Materials Laboratories
Indianapolis, IN 46206

United Aircraft Company
Pratt & Whitney Aircraft Division
East Hartford, CT 06108

United Aircraft Research Lab
East Hartford, CT 06108
Attn: Mr. Roy Fanti

FINAL REPORT ONLY

Defense Documentation Center
Cameron Station
Alexandria, VA 22314
Via: Commander
Naval Air Systems Command
(AIR-50174)
Department of the Navy
Washington, DC 20361
(twelve copies)

NASA
Scientific & Technical Information
Facility
P.O. Box 33
College Park, MD 20740
(one copy)

Titanium Metal Corporation of America
Henderson, Nevada 89015
Attn: Dr. Harry W. Rosenberg

Reactive Metals Inc.
Niles, OH 44446
Attn: Dr. Howard Bomberger

Southwest Research Institute
8500 Culebra
P.O. Box Drawer 28510
San Antonio, TX 78284
Attn: Dr. C. Gerald Cardner

Dr. J. C. Williams
Dept. of Mettalurgy & Materials Science
Carnegie Mellon University
Pittsburgh, PA 15213

Massachusetts Institute of Technology
Dept. of Metallurgy & Materials Science
Cambridge, MA 02139
Attn: Dr. W. A. Backofen
Dr. N. J. Grant
(one copy each)

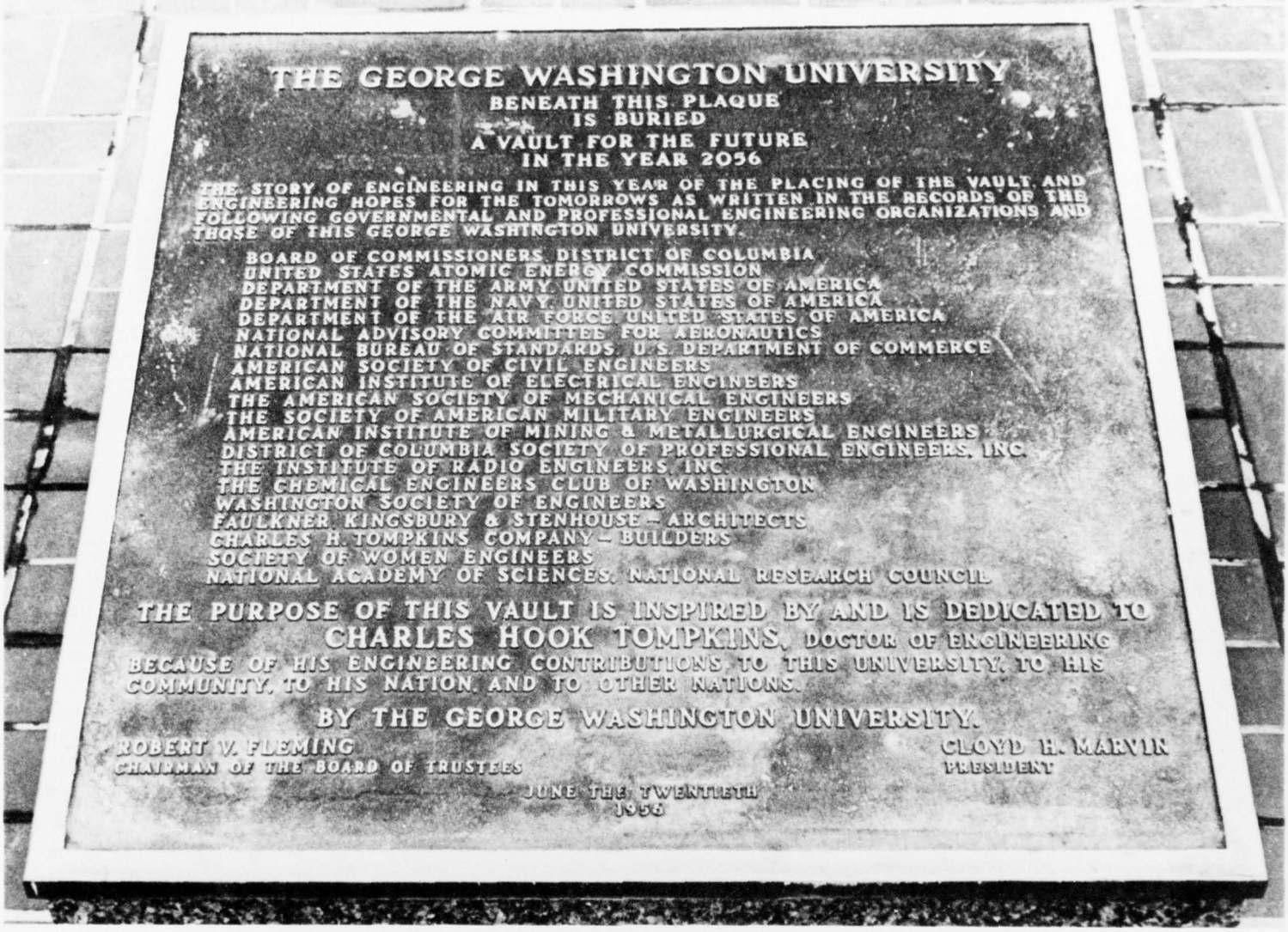

To cope with the expanding technology, our society must be assured of a continuing supply of rigorously trained and educated engineers. The School of Engineering and Applied Science is completely committed to this objective.


FILM
5